Development and characterization of Polycaprolactone/chitosan-based scaffolds for tissue engineering of various organs: A review

Javad Esmaeili, Saeedeh Zare Jalise, Silvia Pisani, Gaël Y Rochefort, Farbod Ghobadinezhad, Zeynab Mirzaei, Riaz Ur Rehman Mohammed, Mehdi Fathi, Amir Tebyani, Zohreh Mousavi Nejad

Development and characterization of Polycaprolactone/chitosan-based scaffolds for tissue engineering of various organs: A review

Javad Esmaeili, Saeedeh Zare Jalise, Silvia Pisani, Gaël Y. Rochefort, Farbod Ghobadinezhad, Zeynab Mirzaei, Riaz Ur Rehman Mohammed, Mehdi Fathi, Amir Tebyani, Zohreh Mousavi Nejad

PII: S0141-8130(24)03746-2

DOI: https://doi.org/10.1016/j.ijbiomac.2024.132941

Reference: BIOMAC 132941

To appear in: *International Journal of Biological Macromolecules*

Received date: 11 January 2024

Revised date: 27 May 2024

Accepted date: 4 June 2024

Please cite this article as: J. Esmaeili, S.Z. Jalise, S. Pisani, et al., Development and characterization of Polycaprolactone/chitosan-based scaffolds for tissue engineering of various organs: A review, *International Journal of Biological Macromolecules* (2023), https://doi.org/10.1016/j.ijbiomac.2024.132941

Development and Characterization of Polycaprolactone/Chitosan-based Scaffolds for Tissue Engineering of Various Organs: A Review

Javad Esmaeili [a, b, c,*], Saeedeh Zare Jalise [d], Silvia Pisani [e], Gaël Y. Rochefort [f, g], Farbod Ghobadinezhad [h], Zeynab Mirzaei [i], Riaz Ur Rehman Mohammed [j], Mehdi Fathi [k], Amir Tebyani [l], Zohreh Mousavi Nejad [m, n]

[a] Department of Chemical Engineering, Faculty of Engineering, Arak University, Arak 38156-88349, Iran-

[b] Department of Tissue Engineering, TISSUEHUB Co., Tehran, Iran.

[c] Tissue Engineering Hub (TEHUB), Universal Scientific Education and Research Network (USERN), Tehran, Iran.

[d] Department of Tissue Engineering and Applied Cell Sciences, School of Medicine, Qom University of Medical Sciences, Qom, Iran.

[e] Department of Drug Sciences, University of Pavia, Via Taramelli 12,27100 Pavia Italy.

[f] Bioengineering Biomodulation and Imaging of the Orofacial Sphere, 2BIOS, faculty of dentistry, tours university, France.

[g] UMR 1253, iBrain, Tours University, France.

[h] USERN office, Kermanshah University of Medical Sciences, Kermanshah, Iran.

[i] Institute for Nanotechnology and Correlative Microscopy e. V. INAM, Forchheim, Germany.

[j] Mechanical and Materials Engineering, University of Nebraska Lincoln.

[k] Department of Esthetic and Restorative Dentistry, School of Dentistry, Ardabil University of Medical Sciences, Ardabil, Iran.

[l] Department of Chemical Engineering, Faculty of Engineering, Tehran University, Tehran, Iran.

[m] School of Mechanical and Manufacturing Engineering, Dublin City University, D09 Y074 Dublin, Ireland.

[n] Centre for medical engineering research, school of mechanical and manufacturing engineering, Dublin city university, D09 Y074 Dublin, Ireland.

***Corresponding**; Javad Esmaeili, Ph.D.; Email: Ja_esmaeili@yahoo.com, Phone: +982188458516.

Abstract

Research in creating 3D structures mirroring the extracellular matrix (ECM) with accurate environmental cues holds paramount significance in biological applications. Biomaterials that replicate ECM properties—mechanical, physicochemical, and biological—emerge as pivotal tools in mimicking ECM behavior. Incorporating synthetic and natural biomaterials is widely used to produce scaffolds suitable for the intended organs. Polycaprolactone (PCL), a synthetic biomaterial, boasts commendable mechanical properties, albeit with relatively modest biological attributes due to its hydrophobic nature. Chitosan (CTS) exhibits strong biological traits but lacks mechanical resilience for complex tissue regeneration. Notably, both PCL and CTS have demonstrated their application in tissue engineering for diverse types of tissues. Their combination across varying PCL:CTS ratios has increased the likelihood of fabricating scaffolds to address defects in sturdy and pliable tissues. This comprehensive analysis aspires to accentuate their distinct attributes within tissue engineering across different organs. The central focus resides in the role of PCL:CTS-based scaffolds, elucidating their contribution to the evolution of advanced functional 3D frameworks tailored for tissue engineering across diverse organs. Moreover, this discourse delves into the considerations pertinent to each organ.

Keywords: Scaffold, Polycaprolactone, Chitosan, tissue engineering, organ, biomaterial

1. Introduction

Tissue engineering, a swiftly advancing domain, endeavors to forge operational substitutes for tissues harmed or impaired by disease. A chief hurdle here involves producing frameworks capable of bolstering cellular proliferation and the transformation into operational tissues. Polycaprolactone (PCL) and chitosan (CTS) stand as two polymers, biocompatible and biodegradable, meticulously scrutinized for their potential role in tissue engineering due to their advantageous physical and biological traits[1]. PCL, a synthetic polymer, touts solid mechanical attributes, allowing facile conversion into assorted configurations encompassing porous scaffolds. Conversely, chitosan, a natural polymer sourced from chitin, has showcased antimicrobial and anti-inflammatory traits[2]. These composites can be fabricated and tailored to

fit the specific needs of different tissues and organs. Additionally, PCL-CTS scaffolds can be combined with other materials and technologies to enhance their regenerative capabilities. The addition of CTS to PCL allows for the modulation of the physicochemical properties of the scaffolds, leading to highly porous constructs with distinct morphologic and mechanical features.

In recent years, scaffolds founded on PCL and CTS have emerged as an encouraging stage for tissue engineering **(Table 2)**. This involves the utilization of scaffolds based on PCL and CTS. These scaffolds have proven to be a significant platform for engineering various organs. This includes hard tissues such as bone, characterized by their high load-bearing capacity. On the other hand, they also include soft tissues like the lungs and skin, which are typically non-load-bearing. Various techniques, such as freeze-drying, electrospinning, and 3D printing, are harnessed to fabricate these scaffolds, which can be modified to incorporate bioactive molecules fostering tissue revival[3]. This exploration delves into the latest strides in PCL/CTS-based scaffold innovation, exploring diverse tissue engineering prospects. Emphasis rests on the crafting, characterization, and biological efficacy of these structures[4].

The scaffolds function as host materials that nurture incubating cells, steering their adherence, expansion, transformation, reproduction, phenotype, and migration to foster fresh tissue emergence[5]. One of the prime challenges in tissue engineering revolves around formulating scaffolds adept at backing cell maturation into functional tissues. The quest to produce clinically pertinent engineered tissue necessitates precise cell selection and sourcing criteria, accounting for accessibility with minimal invasiveness. Tissue engineering has undergone significant evolution lately, with a noticeable focus on using adult stem cells.

Table 1- PCL-CTS nanofiber production[6].

Formulation (% w/v)	**Needle gauge**	**Flow rate (µL/min)**	**Fiber diameter (nm)**
PCL 5%	22G	10	88±46
		25	57±33
PCL 10%	22G	10	344 ±92
		25	357±262

PCL 5% + Chitosan	22G	10	95± 18
		25	87±31
PCL 10% + Chitosan	22G	10	151 ±35
		25	102± 21
PCL 15% + Chitosan	22G	10	Solution dried too quickly at all flow rates to be usable
		25	

The degradation products and toxicity of PCL and CTS composites have been studied in several papers. CTS is a natural polymer with potential biomedical applications, including drug delivery systems and tissue engineering. Scientific evaluations conducted via computational methods have revealed intriguing findings. CTS-oligomers, the byproducts of chitosan degradation, exhibit pharmacological properties that hold significant promise. These properties are observed irrespective of their molecular weight, degree of deacetylation, and acetylation pattern. Importantly, these CTS-oligomers demonstrate minimal toxicity in human subjects[7]. PCL-CTS membranes have also been evaluated for their degradation and biocompatibility properties, showing satisfactory results for application in wound repair[8]. Porous scaffolds made from PCL-CTS blends have been prepared and characterized, with stability and pore morphology dependent on the relative mass ratio of the two polymers. These scaffolds were found to be non-toxic to vasculature[9]. A composite membrane combining chitosan and beta-dicalcium pyrophosphate (beta-DCP) ceramic particles has been evaluated for biodegradation behavior and cytotoxicity, showing potential as a cell substrate in tissue engineering[10].

The blend ratio of PCL and CTS has been found to affect the properties of the composite materials significantly[11]. These composites have been used to prepare membranes with desirable properties such as thermal stability, hydrophilicity, and mechanical viscoelasticity[12]. The 10:90 (w/w) blend ratio of PCL-CTS has been recommended as the optimum ratio for tissue engineering applications[13]. Chitosan and its composites have shown great potential in tissue regeneration and artificial organ research[14]. Chitosan derivatives have been synthesized for various applications in biological engineering, including cardiac, liver, and wound healing[15]Additionally, PCL and chitosan have been used to develop scaffolds for tissue

engineering applications with faster degradation rates, hydrophilicity, and porosity. PCL and chitosan composites have demonstrated promising applications in various organs and tissues in tissue engineering and biomedical research (Figure 1**)**.

Table 2- A brief description of some studies focusing on using PCL/chitosan for tissue engineering of different organs.

Organs	Fabrication Technique	**Additive (Drug, Growth Factor)**	In Vitro (**Cell**)	In Vivo (**Animal**)	**Mechanical Properties (Elastic Or Compression Module)** (Mpa)	**Swelling** %	Cell Viability %	**Porosity** %	**Ref**.
Skin	Electrospinning	-	Mouse Fibroblast (L-929) Cell Line	-	12.41	150	100	-	[16]
Skin	Electrospinning	-	-	Balb/c mice	5.25	-	-	-	[17]
Skin	Electrospinning	Fucoidan	Fibroblasts	-	22.74	38.27	100	-	[18]
Bone	Melt Stretching And Multilayer Deposition	-	MC3T3-E1 Cell	-	12-15	30-55	>90	45.99	[19]
Bone	Electrospinning	-	MC3T3-E1 Cell	-	-	-	100	-	[20]
Cartilage	3D Printing	-	Rabbit Articular Chondrocytes	rabbit	-	-	>89	-	[21]
Menisci	3D Printing	-	Hadscs,	-	4-6	-	>90	17-85	[22]
Blood vessels	Electrospinning	-	Endothelial	-	2.3	-	>95	-	[23]
Blood vessels	Electrospinning	-	Endothelial	Pig	-	-	100	80	[24]
Blood vessels	Electrospinning	Collagen	Endothelial	-	3.5	-	>95	-	[25]
Muscles	Electrospinning	Norepinephrine	Skeletal Muscle Cell Line L6	mice	>3	-	80	-	[26]
myocardium tissue	Disk Molding		Wharton's Jelly Mesenchymal Stem Cells		<1	-	>85	-	[27]
Eye	Solvent Casting	Chitosan Nanoparticles	Hcecs	-	-	61	95	-	[28]

retinal	Electrospinning	$SrAl_2O_4$: Eu^{2+}, Dy^{3+}	Retinal Neural Cells	-	1	-	>90	-	[29]
Lung	Electrospinning	-	Porcine Tracheobronchial Epithelial (PTBE)	-	8-33	-	100	-	[30]
Liver	Electrospinning	-	Hepa 1-6 Epithelial Liver Mouse Cells	-	7-8	-	>90	65-87	[1]
Liver	Gelation	-	Human Hepatoma Cell Line Hepg2 Cells	-	0.2-0.7	-	>95	-	[31]
Kidney	Vascular Corrosion Casting Technique	-	Human Renal Cells	rat	-	-	100	-	[32]
Nerve	Electrospinning	-	Schwann Cell	-	65.5	-	>94	-	[33]
Bladder	Molding	Adipose-Derived Stem Cells (Ascs)	Adipose-Derived Stem Cells (Ascs)	rat	-	-	100	90	[34]
Dental	Electrospinning	Polyglycerol Sebacate And Eta Tri-Calcium Phosphate	Human Fetal Osteoblasts (Hfob) Cells	-	16.6	-	>95	-	[35]
Oral cavity	3D Printing	Ibuprofen	Mouse Fibroblast L-929	-	4-10	-	>90	-	[36]
Esophagus	Molding	-	Adult Dermal Fibroblasts	pig	3-5	-	>97	81-85	[37]
Esophagus	Electrospinning	-	Adult Dermal Fibroblasts	-	0.4-5	-	>90	-	[38]
Stomach	Molding	-	Enterocytes	-	-	-	>90	-	[39]
Intestine	Electrospinning	Fe_3O_4	-	-	90-206	-	-	44-47	[40]

In light of the current scientific literature and the importance of these two substances in the field of tissue engineering, a thorough review paper is needed. This paper should study this composite and its utilization in various organs. The investigation should focus on the characteristics and uses of these two substances when combined to form a composite.

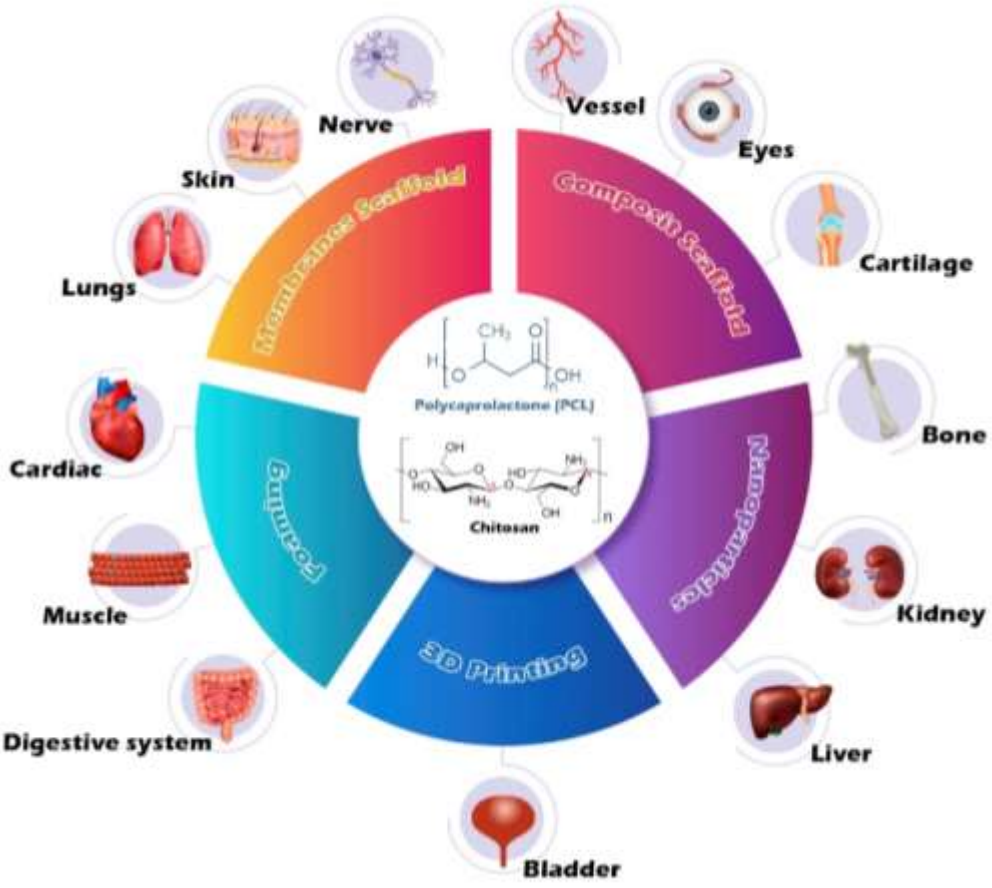

Figure 1: Schematic diagrams encompassing the features of PCL/CTS scaffolds and various tissue engineering applications.

2. Types of PCL/CTS tissue engineering scaffolds

2.1. 3D-printing scaffolds

PCL and CTS have been used in various forms for 3D printing applications. The combination of PCL and CTS in 3D printing allows for the creation of scaffolds with suitable microarchitecture, high efficiency, and high precision[41]. These composite scaffolds have shown promise in bone repair and regenerative applications. Additionally, integrating other biomaterials, drugs, growth factors, and cells with PCL composites further improves their properties and aids bone healing.

PCL has been blended with acetylated chitosan (AC) to create composite materials for tissue engineering[42]. PCL has also been mixed with chitosan or β-tricalcium phosphate (TCP) to fabricate scaffolds for bone regeneration[43]. Chitosan has been combined with pectin to develop hydrogels for 3D printing[44]. Additionally, PCL has been blended with chitosan or coated with chitosan to create scaffolds with improved bioactivity and cell compatibility[45]. Chitosan has also been combined with polyvinyl alcohol (PVA) to create a double-network (DN) hydrogel scaffold for 3D printing[46]. These studies demonstrate the versatility of PCL and chitosan in different forms for 3D printing applications in tissue engineering and regenerative medicine.

2.2. Foaming scaffolds microspheres

Foaming scaffold microspheres from PCL and CTS offer several advantages. Firstly, they enable cell growth and differentiation, making them suitable for tissue regeneration applications[47]. Secondly, these scaffolds have improved biomechanical properties, such as increased viscoelasticity, essential for supporting tissue growth and function[48]. Thirdly, incorporating chitosan microparticles in the scaffolds allows for sustained release of bioactive molecules, such as dexamethasone and ascorbic acid, which can enhance osteogenic differentiation of stem cells[49]. Additionally, chitosan nanofibers in the scaffolds enhance their compressive modulus and water uptake ability, making them more suitable for cell proliferation and tissue integration[50]. Overall, foaming scaffold microspheres from PCL and CTS offer a promising platform for tissue engineering applications, particularly in cartilage and bone regeneration. It has been investigated in several studies. Filová et al. developed foam scaffolds from PCL with incorporated chitosan microparticles, showing that scaffolds with 10 wt% PCL and 0 wt% or 10 wt% CTS are potential scaffolds for cartilage regeneration[47]. Omidvar et al. encapsulated dexamethasone within chitosan microspheres embedded in a fibrous structure of PCL, creating a bilayer fibrous scaffold. The chitosan microspheres acted as depots for the sustained release of dexamethasone, enhancing the proliferation and osteogenic differentiation of human mesenchymal stem cells[48]. Jing et al. produced biomimetic porous PCL scaffolds containing chitosan nanofibers, which improved water uptake ability and biocompatibility, leading to better cell proliferation[51]. Kosowska et al. analyzed the foaming process of PCL-based composite materials, including chitosan, and demonstrated their biocompatibility and suitability for bone cell culture[52]. Virgilio

et al. developed a solvent-free PLA scaffold with chitosan-grafted PLA copolymer, which enhanced cell proliferation when immobilized on the surface of the pores[28].

2.3. Nanoparticles

Nanoparticles from PCL and CTS offer several advantages. They can be used as drug delivery systems, enhancing the efficacy of encapsulated drugs and improving their interaction with target cells[53]. CTS nanoparticles can encapsulate and transport drugs within the body, improving the bioavailability and therapeutic effect of the drugs[54]. Additionally, CTS nanoparticles can be used for oral drug delivery, overcoming challenges such as low solubility and poor bioavailability[55]. For various applications, PCL and CTS nanoparticles can also be incorporated into composite materials, such as membranes and scaffolds. These composite materials exhibit good dispersion of nanoparticles, stability, and efficiency, making them suitable for renewable energy systems and tissue engineering, such as organic photovoltaic solar cells and bone tissue engineering[49]. Overall, nanoparticles from PCL and CTS offer versatile and promising options for drug delivery and tissue engineering applications.

Nanoparticles have been used in the development of PCL and CTS-based scaffolds for tissue engineering applications[56]. Chitosan-dextran nanoparticles loaded with transforming growth factor-beta 1 (TGF-β1) were incorporated into a nanofiber scaffold composed of PCL and poly-l-lactic acid (PLLA)[53]. These scaffolds showed high porosity, mechanical properties, and sustained release of TGF-β1, which promoted the expression of genes related to cartilage tissue engineering[57]. In another study, biodegradable polycaprolactone nanoparticles (PCL-NPs) were developed for the Osimertinib Mesylate (OSM) active targeting in lung cancer treatment[55]. Chitosan-fabricated OSM-loaded PCL-NPs showed improved anticancer efficacy and reduced side effects[58]. Chitosan nanoparticles (ChNs) have also been optimized for size and zeta potential by varying chitosan molecular weight, concentration, and stirring speed. Composite membranes of polysulfone and chitosan incorporated with nickel-zinc ferrite and magnetite nanoparticles have been synthesized for applications in organic photovoltaic solar cells. Chitosan-based nanoparticles have a wide range of applications in drug delivery, gene delivery, and antimicrobial activity.

2.4. Membrane scaffolds

Membrane scaffolds made from a blend of PCL and CTS offer several advantages. Firstly, they provide a suitable microenvironment for the incorporation of cells or growth factors, making them highly useful for tissue engineering and regenerative medicine applications[59]. Secondly, these scaffolds have a highly porous structure with interconnected pore networks, allowing for easy cell invasion, viability, and transfer of essential nutrients, oxygen, and growth factors[60]. Thirdly, the presence of chitosan in the blend increases the porosity of the membrane, enhancing cell proliferation and oxygen uptake[61]. Additionally, PCL-CTS blend membranes have been shown to have remarkable wound-healing properties, making them effective as wound-dressing materials[12]. Furthermore, these membranes have been successfully used for culturing corneal endothelial cells, promoting cell adhesion and proliferation, and maintaining cell phenotype[62]. PCL-CTS blend membranes offer biocompatibility, transparency, and biodegradability, making them suitable for various tissue engineering applications. Various ratios of PCL-CTS blend membranes have been prepared and characterized[59]. The PCL and CTS blend ratio significantly affects the membranes' thermal stability, hydrophilicity, and mechanical properties. The best blend ratio for PCL-CTS membranes is 10:90 (w/w)[12]. Chitosan nanoparticles (CSNPs) have been incorporated into PCL-CTS membranes to create a transparent scaffold for culturing corneal endothelial cells. Increasing the CSNP/PCL ratio improves the transparency and surface wettability of the scaffold[61]. A novel copolymer synthesis of Di isopropyl fumarate (F), vinyl benzoate (V), and 2-hydroxyethyl methacrylate (H) has been developed for membrane design. The terpolymer obtained, along with chitosan, shows potential for use in regenerative medicine[16]. Electrospun fibrous membranes of PCL and polyvinylpyrrolidone (PVP) have been produced, and a blend of collagen/chitosan has been grafted onto the surface. These membranes show promise for application in skin tissue engineering[62].

2.5. Composite scaffold

Composite scaffolds made from a combination of PCL and CTS offer several advantages. Firstly, PCL-CTS blend scaffolds fabricated through wet electrospinning have shown to be highly effective wound dressing materials with remarkable wound healing properties[60]. Secondly, composite dressings made from chitosan sponge and PCL nanofibrous membrane with

asymmetric wettability surfaces have demonstrated excellent cytocompatibility, vapor transmission rate, and liquid absorption, making them a promising alternative to traditional wound dressings[17]. Thirdly, PCL-CTS scaffolds functionalized with Mytilus californiensis protein have shown superior bioactivity and cellular proliferation properties, making them attractive for bone regeneration applications[18]. Lastly, composite scaffolds made from PCL and CTS, either through blending or surface coating techniques, have shown enhanced cell attachment, proliferation, and upregulation of bone markers, making them effective for tissue engineering applications[45]. It has been investigated in several studies. One study fabricated a tri-polymer scaffold using PCL-gelatin-CTS through electrospinning, which showed potential for bone tissue engineering (Gautam et al.[63]). Another study designed a composite dressing with a chitosan sponge and PCL nanofibrous membrane, which exhibited asymmetric wettability surfaces and had potential as a wound healing material (Yang et al.[17]). A third study evaluated the properties of PCL-CTS scaffolds functionalized with Mytilus californiensis protein, showing superior properties in terms of bioactivity and cellular proliferation (Rojas-Yañez et al.[18]). Additionally, a study compared blended scaffolds (PCL-CTS) with scaffolds fabricated using surface coating technique (PCL-CTS), and found that the surface-coated scaffolds exhibited enhanced cell attachment, proliferation, and bone marker upregulation (Poddar et al.[45]). Finally, a study synthesized composite materials loaded with recycled porcine bone powder using PCL and CTS as matrices, demonstrating suitable mechanical properties for hard tissue engineering applications (Valente et al.[64]).

3. PCL-CTS-based scaffolds for tissue engineering of organs

3.1. Skin

Skin tissue engineering was one of the first organ systems targeted by regenerative medicine techniques[65]. Autologous skin grafting remains the gold standard for treating deep second and third-degree burns. However, much of the research in skin tissue engineering is focused on developing 3D polymer scaffolds that incorporate biomolecules and cells. These scaffolds provide a supportive structure for the growth and differentiation of cells into functional skin tissue, aiming to improve the treatment of burns and other skin injuries [66]. The use of advanced fabrication techniques, such as 3D printing, has enabled the creation of complex scaffold architectures that mimic the structure of native skin tissue, while the incorporation of bioactive

molecules and cells can enhance tissue regeneration and promote healing[67]. This is an exciting area of research with the potential to improve patient outcomes significantly.

Prasad et al. [68] PCL-CTS blend electrospun mats were prepared and characterized physiochemically and biologically compared to electrospun PCL scaffolds. The results showed that the PCL-CTS scaffolds exhibited enhanced hydrophilicity, swelling behavior, mechanical performance, and thermal stability. Additionally, these blend fibers improved the activities of keratinocytes and L-929 cell lines and the distribution of actin on the scaffolds. In conclusion, the PCL-CTS blend fibers were a superior scaffold for skin tissue engineering compared to PCL fibers alone.

In another study, the in vivo effects of electrospun PCL-CTS nanofibers on wound healing were tested by creating cutaneous excisional skin defects in mice **(Figure 2A)**. The results were compared to those obtained using Tegaderm, a commercial wound dressing. Gross and histological assessments indicated that the wounds treated with PCL-CTS nanofibers exhibited improved closure and more biomimetic healing. As a result, electrospun PCL-CTS mats have the potential to serve as a biomimetic replacement for natural extracellular matrix (ECM) and may be used as scaffolds for skin tissue engineering. In future studies, these mats may also be used to deliver cells and proteins to skin defects[69]. Jung et al.[70] A composite of CTS nanoparticles and electrospun PCL fibers was fabricated for wound dressing applications and drug delivery to skin tissue. Various assessments of these complexes demonstrated no cytotoxicity and beneficial penetration of the CTS nanoparticles into rat primary fibroblasts. Results from SEM, FITC, and MTT assays indicated the potential of these composites to be used as drug carriers for wound healing without causing any side effects. These findings suggest that combining CTS nanoparticles and electrospun PCL fibers may offer a promising approach for developing advanced wound dressings and drug delivery systems for skin tissue.

In a study by Ozkan et al., core-shell scaffolds were developed through the coaxial electrospinning of CTS as the shell and PCL as the core. Microscopy methods confirmed the optimized core-shell structure, while antibacterial tests showed that the antibacterial effect of these complex scaffolds on E. coli and S. aureus was similar to that of pure CTS. In vitro, biodegradability tests indicated that the scaffolds maintained their biodegradability. These results

suggest that these structures have the potential to be used as beneficial substrates for wound healing and skin tissue engineering[71].

Chen et al.[72] CTS-graft-PCL was synthesized using ring-opening polymerization by grafting ε-caprolactone oligomers to the CTS hydroxyl groups. Electrospun fibers were then prepared by combining this graft copolymer with PCL. The resulting fibrous scaffolds were characterized using X-ray photoelectron spectroscopy (XPS), SEM, and zeta-potentiometry. In vitro studies using mouse fibroblasts demonstrated that CTS-graft-PCL/PCL scaffolds with a ratio of 2 to 8 had the best performance as skin tissue engineering scaffolds, as they could promote cell activities more than other prepared scaffolds with different ratios. These findings suggest that combining CTS-graft-PCL and PCL may offer a promising approach to developing advanced scaffolds for skin tissue engineering.

3.2. Bone

Despite its limitations, including a sluggish biodegradation rate and inherent hydrophobicity, PCL has found extensive application in tissue engineering. The reasons for this widespread use are manifold. They include its mechanical robustness, its compatibility with biological systems, the simplicity of its processing, and its ability to degrade over time[19, 73]. Furthermore, PCL is an FDA-approved polymer used in tissue engineering applications currently used as an implant and scaffold material. PCL possesses mechanical properties similar to bone and has a controlled biodegradation ability, making it a promising candidate for use in bone tissue engineering. These properties, combined with its approval for use in medical applications, make PCL a valuable material for the development of advanced tissue engineering scaffolds[74].

CTS is a biopolymer known for its excellent hydrophilicity, biodegradability, and biocompatibility, although its mechanical properties are inferior[75, 76]. Several studies[20, 77, 78] have reported that CTS promotes bone mineralization, osteoblast differentiation, and growth in vivo. The strong attraction between the positively charged CTS surface and the negatively charged cell surface is thought to increase the metabolic activity of cells[79]. Additionally, the structure of CTS mimics glycosaminoglycans (GAGs) of the extracellular matrix (ECM), which can facilitate the adhesion and proliferation of osteoblasts. By combining the biopolymer CTS with the synthetic polymer PCL, it is possible to take advantage of both the excellent biological attributes of CTS

and the physicochemical properties of PCL. As a result, a mixture of PCL and CTS may be a promising candidate for use in bone tissue engineering.

In 2011, Thuaksuban et al. used a home-developed method called melt stretching and multilayer deposition (MSMD) to fabricate PCL-CTS scaffolds[79]. The process involved melting and stretching to produce monofilaments of PCL-CTS containing 0, 10, 20, and 30 wt% CTS. These filaments were then arranged and deposited to create multilayer 3D scaffolds. Physical and biological evaluations showed that the best results were obtained with the PCL-20%CTS scaffold. This approach demonstrates the potential of using advanced fabrication techniques to create complex scaffold architectures for tissue engineering applications.

Nanofibrous PCL-CTS membranes have recently gained significant attention in the field of bone tissue engineering due to their unique properties, such as high surface area and the ability to mimic the ECM[80]. In a recently published study [81], Zhu et al. designed and developed a metformin-loaded PCL-CTS electrospun membrane to use as a guided bone regeneration barrier membrane **(Figure 2B)**. The results of this study showed that the presence of metformin enhanced osteogenic mineralization and alkaline phosphatase activity in bone marrow stromal cells[82-84]. In another study [85], Jhala et al. fabricated a PCL-CTS nanofibrous scaffold with an average diameter of approximately 75 nm, which induced early osteogenic differentiation in MC3T3-E1 pre-osteoblasts. These findings demonstrate the potential of PCL-CTS nanofibrous scaffolds for bone tissue engineering applications.

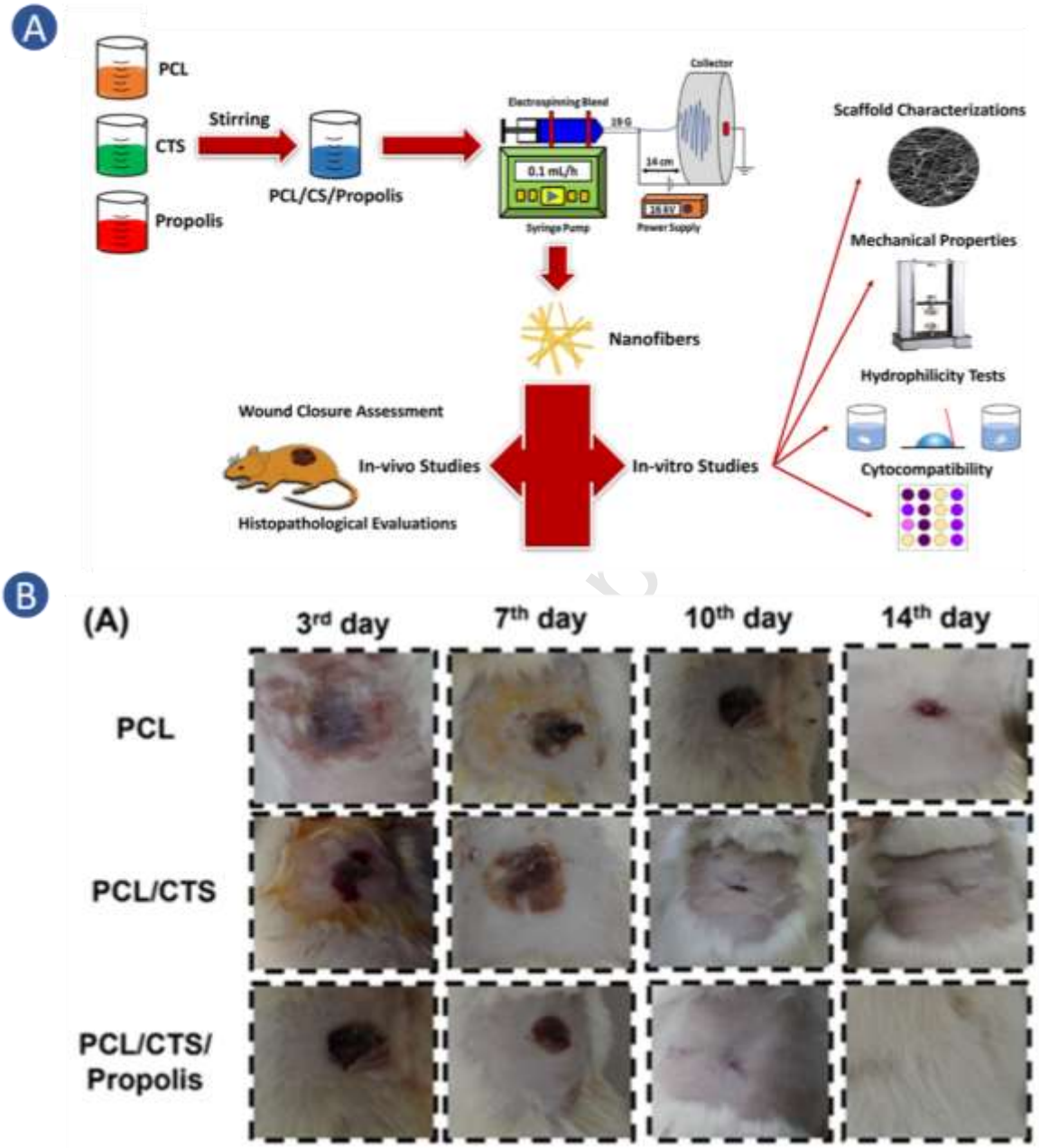

Figure 2: A) Development and assessment of a fibrous nanocomposite scaffold made from polycaprolactone, chitosan, and propolis for use as a skin substitute in tissue engineering[86], **B)** Microphotographs and the corresponding SEM images of cells on PCL/CTS bioscaffold for 48 h **(a1–a4)**, 96 h **(b1–b4),** and on PCL/CTS/SiO2 bioscaffold for 48 h **(c1–c4)**, 96 h **(d1–d4)**[87].

One effective approach in bone tissue engineering is using 3D scaffolds, which provide a suitable environment for the growth of bone cells[22, 88]. The porosity of these scaffolds is critical, and fabrication methods capable of creating highly porous scaffolds, such as freeze-drying, are often used[76, 89]. Chong et al. [90] fabricated PCL-CTS sponge-like 3D scaffolds using the freeze-

drying technique to address one of the significant drawbacks of PCL: its lack of cell-recognition signals. The resulting scaffolds were homogeneous porous structures with enhanced hydrophilic properties. In another research [91], PCL-CTS 3D porous scaffolds with a unique honeycomb-like structure were fabricated using the phase separation method. These scaffolds had a high volume of porosity, ranging from 80% to 90%, and good interconnectivity, making them promising candidates for use in bone tissue engineering applications.

Surface treatment methods, such as coating with CTS, can be effective in improving cell recognition in PCL-based scaffolds[92]. According to a recent publication [93], successfully coated CTS onto the pore walls of a 3D PCL-based scaffold using a modified porogen leaching method. This study aimed to enhance the biocompatibility and osteoconductivity of the PCL scaffolds by applying a CTS coating to the interior pore walls. According to the biological evaluation results, the scaffold coated with 2.5% (w/v) CTS had the highest cell viability, biocompatibility, and osteoblast differentiation, making it a promising candidate for bone regeneration scaffold. This approach demonstrates the potential of using surface treatments to improve the performance of PCL-based scaffolds in tissue engineering applications.

3.3. Cartilage

In a study by Neves et al. [94] CTS-PCL scaffolds were fabricated as 3D fiber meshes using wet-spinning and folding the fibers into cylindrical molds, followed by thermal treatment. The homogeneity of PCL throughout the CTS phase was confirmed using differential scanning calorimetry (DSC) and Fourier-transform infrared spectroscopy (FTIR). Micro-computed tomography (μCT) analysis revealed suitable interconnected pores and pore size, meeting the desired porosity for cartilage tissue engineering scaffolds. Furthermore, after 21 days of culture with bovine articular chondrocytes, the scaffolds showed the formation of a cartilaginous extracellular matrix and the production of glycosaminoglycans (GAGs) (Figure 3**A)**. Scaffolds with a 75 wt% content of CTS exhibited the best cell activity and cartilaginous extracellular matrix formation. These findings demonstrate the potential of PCL-CTS scaffolds for use in cartilage tissue engineering applications **(Figure 3B)**.

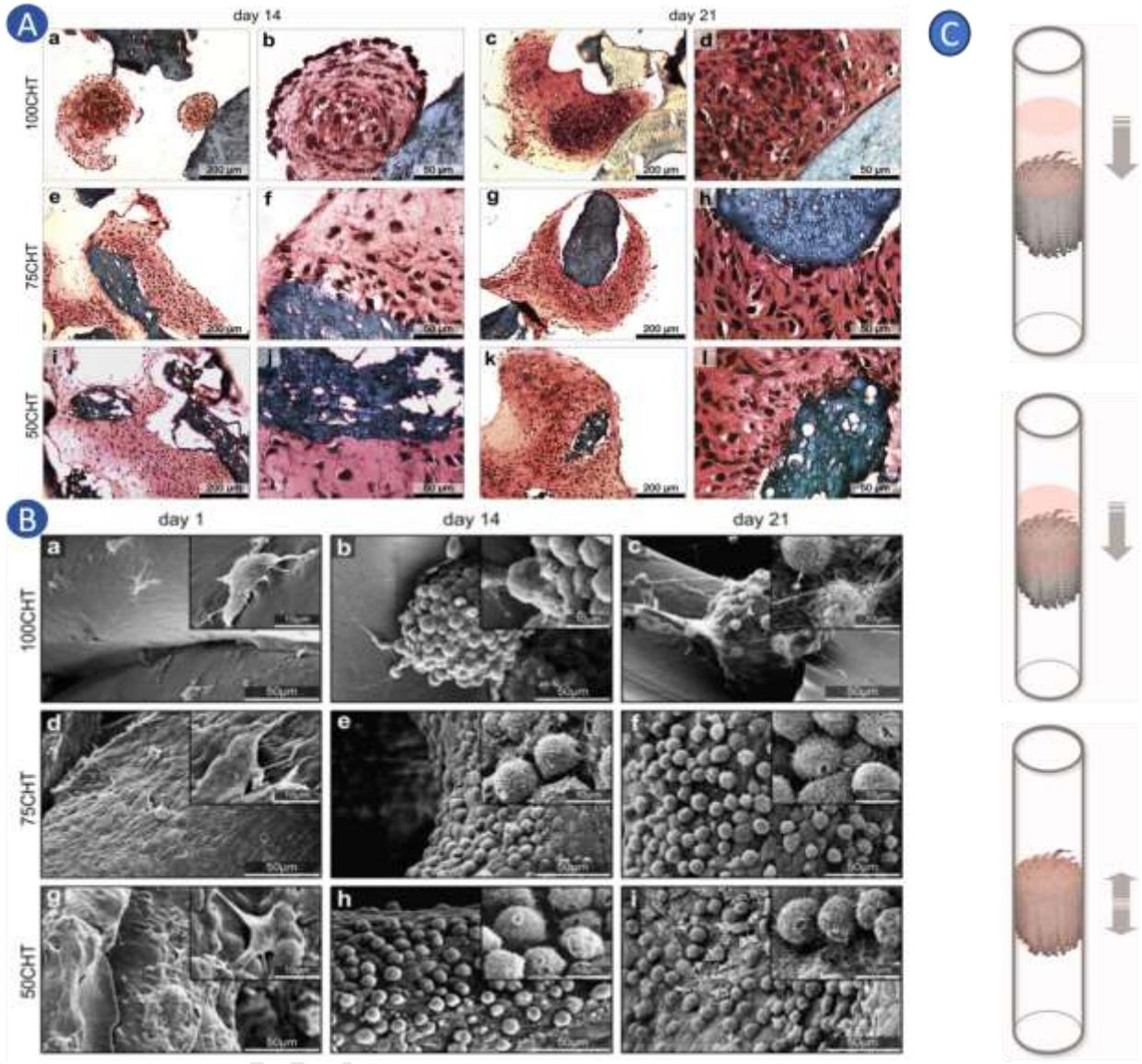

Figure 3: A) Histological cross-sections show GAGs production (stained red) on the (aed) 100CHT, (eeh) 75CHT, and (iel) 50CHT scaffolds on day 14 **(a, b, e, f, i, j)** and day 21 **(c, d, g, h, k, l)** of culture in differentiation medium, by safranin-O staining. The dark spots and bluish regions represent cells corresponding to the scaffold material and, **B)** SEM micrographs showing chondrocytes distribution and morphology over the scaffold fibers surface after 1 **(a, d, g)**, 14 **(b, e, h)** and 21 **(c, f, i)** days in culture, with differentiation medium. Cell density: 5 105 cells/20 Ml [94]. **C)** The movement of the cell suspension through the scaffold is facilitated by gravity. Finally, the scaffold was physically rotated along the lengthwise axis to ensure an even distribution of cells[95].

In another study, Abuelreich et al. produced a combination of nanofibrous scaffolds composed of CTS and PCL using an innovative mixing electrospinning technique. To investigate the chondrocyte differentiation of mesenchymal stem cells (MSCs), the human cell line hTERT-MSC-CL1 was cultured on the scaffolds**.** Differentiation of these cells into higher-level cells, such as chondrocytes, was demonstrated through various molecular and staining assays. These

findings suggest combining CTS and PCL in nanofibrous scaffolds may offer a promising approach for promoting chondrocyte differentiation in tissue engineering applications[4].

In a study by Schagemann et al., hybrid scaffolds were developed by combining a microporous PCL matrix, created using computerized rapid prototyping (RP), with a CTS solution through immersion and freeze-drying for 36 hours. When rabbit articular chondrocytes were cultured on these hybrid constructs **(Figure 3C),** histological analysis and various staining methods indicated neocartilage formation, suggesting that these scaffolds have great potential for cartilage tissue engineering applications. Adding CTS to the PCL matrix improved its biomimetic properties and enhanced its bioactive interactions with chondrogenic cells. These findings demonstrate the potential of combining PCL and CTS to create advanced scaffolds for cartilage tissue engineering[95].

3.4. Menisci

The meniscus is a fibrocartilaginous structure located in the knee between the femur and tibia, providing cushioning when a load is applied to the knee. It has a heterogeneous structure, resulting in complex physical properties. The meniscus consists of two components: medial and lateral. The medial component is avascular, while the lateral part is well-vascularized but susceptible to injury due to poor blood perfusion. The meniscus resists axial compression with an aggregate modulus of 100-150 kPa and a tensile modulus of 100-300 MPa circumferentially and 10-30 MPa radially. Its shear modulus is approximately 120 kPa, indicating that the meniscal tissue is anisotropic. Therefore, any scaffold designed to regenerate or repair the meniscus must incorporate this heterogeneity. Currently, multiple materials are combined to fabricate scaffolds for the knee meniscus to create a heterogeneous local environment[96].

The mechanical properties of the meniscal scaffolds can be enhanced by one of the following mechanisms:

- Compaction
- Deposition
- Alignment

The mechanisms in question operate on a variety of principles. These include shearing, a process involving the application of opposing forces that cause layers or parts to slide against each other.

Another is direct compression, which consists of applying force to reduce the size or change the shape of an object. Ultrasound, a method that uses high-frequency sound waves, is another principle. Fluid perfusion, which involves fluid passage through the circulatory system or a specific organ, is also a key mechanism. Lastly, hydrostatic pressure, the pressure exerted by a fluid at equilibrium due to the force of gravity, is another fundamental principle these mechanisms are based on[97].

An ideal scaffold for meniscal regeneration must possess the following mechanical properties:

- Compressive modulus: 75-150 kPa
- Tensile modulus: 75-150 MPa

The above properties can be incorporated by using a blend of different materials. PCL is often used for meniscus regeneration owing to its mechanical properties. However, adding CTS improves the scaffold's biocompatibility and is strongly preferred[98].

In a study by Asgarpour et al.[99], PCL scaffolds with different strand spaces were fabricated using 3D bioprinting via fused deposition modeling. The scaffolds with a strand space of 0.2 mm were modified with CTS by immersing the scaffold in pure CTS solution for 10 seconds. Mechanical tests on the scaffolds showed that the PCL (0.2%) scaffold survived greater force and had a higher modulus than the PCL(0.4%) scaffold, with a compressive modulus of 6-57 MPa. When incubated with human adipose-derived stem cells (hADSCs), SEM images showed cell attachment and normal cell morphology. The MTS assay indicated increased metabolic activity over time. These results and cellular assays suggest that the PCL-CTS scaffolds are suitable for meniscal regeneration. Furthermore, when these scaffolds were combined with natural extracellular matrix extracted from sheep meniscus, hADSCs differentiated into fibroblasts, as evidenced by the expression of chondrogenic and meniscal ECM genes such as SOX9, COLL2, and ACAN **(Figure 4B)**[99].

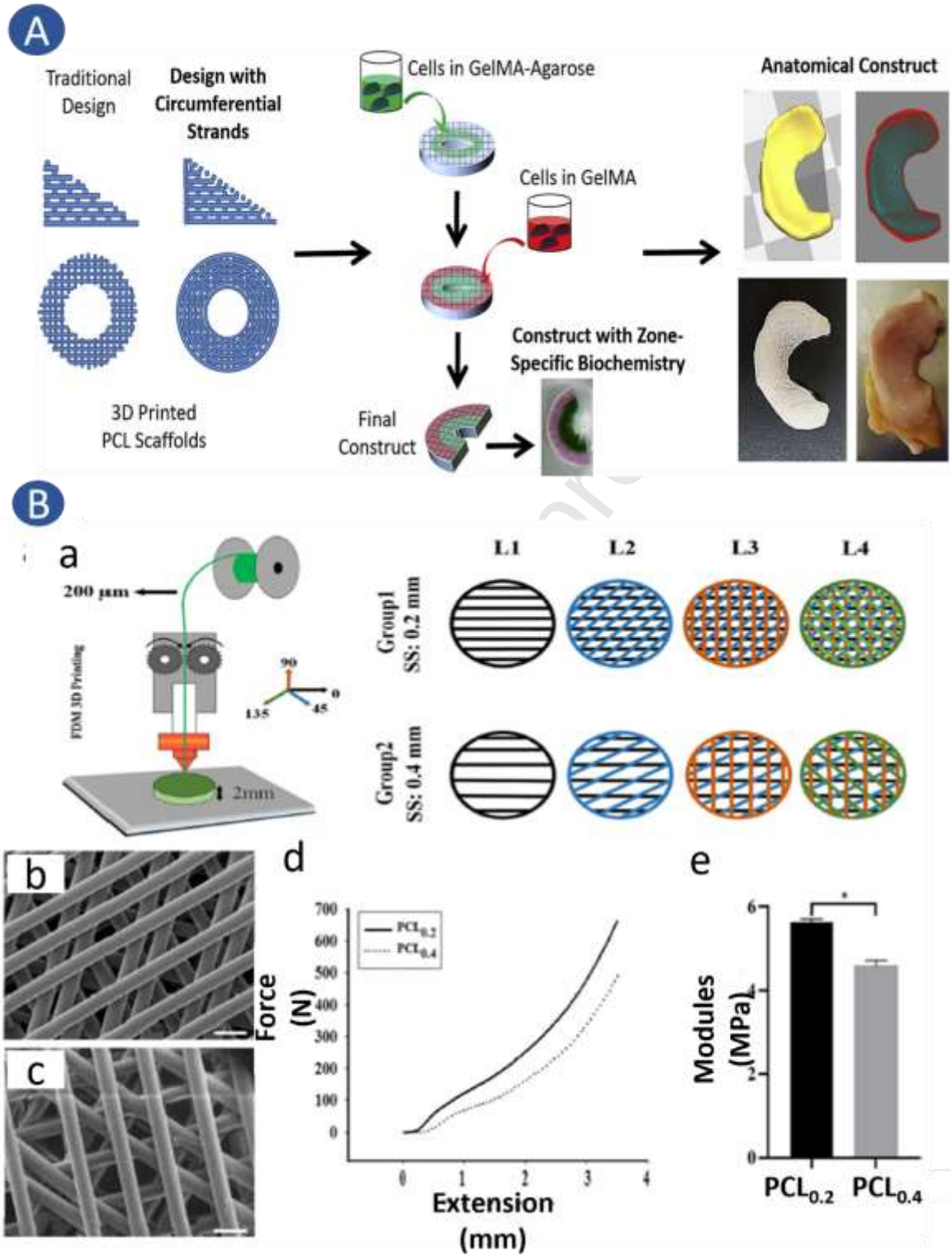

Figure 4: A) A meniscus construct that is anatomically designed with a specific biochemical composition and structural structure based on different zones[100]. **B) (a)** FDM printing setup and scaffold construction for PCL(0.2%) and PCL(0.4%), **(b)** SEM image of PCL(0.2%), **(c)** SEM image of PCL(0.4%) (scale bar: 100 um), **(d)** Compression force-extension curves, and **(e)** Modulus of OCL(0.2%) and PCL(0.4%).

Numerous efforts have been made to create scaffolds that closely mimic the native environment of the human meniscus **(Figure 4A)** [100]. Researchers have utilized PCL-based scaffolds, hydrogel scaffolds, and PLLA-PLGA copolymer scaffolds[96]. Several studies have reported using PCL-CTS scaffolds for various soft tissues, but not many have focused on meniscal regeneration. The flexibility and superiority of the PCL-CTS blend make it a suitable candidate for meniscal regeneration, as its physical properties can be tuned by controlling the PCL/CTS ratio. This allows for the creation of scaffolds with tailored properties to support the growth and differentiation of cells into functional meniscal tissue.

3.5. Vessel

The arterial vessel wall comprises three distinct concentric layers, each with a unique cellular and matrix composition. From the inner vascular lumen to the outer periphery, these layers are the intima, which is immediately adjacent to the vascular lumen; the media, the intermediate layer; and the adventitia, the outermost layer. Two concentric layers of elastin separate these three layers: the internal elastic lamina, which separates the intima from the media, and the external elastic lamina, which separates the media from the adventitia. These layers work together to provide structure and support to the arterial vessel wall[101, 102].

Like all other organs, the cells of blood vessels require nutrients and oxygen and must expel waste products. Vascular cells often exchange these substances directly with the circulating blood. However, in larger-diameter vessels, the nutrition of the cells that make up the vascular wall can be provided by the blood circulating in the vessel and a capillary system called the vasa vasorum. This capillary network brings nutrients to cells farthest from the vascular lumen and is present in all arteries with more than 29 lamellar units. The vasa vasorum can also deliver various mediators and hormones into close contact with the smooth muscle cells of larger arteries[101].

In the field of tissue regeneration and engineering, the creation of artificial blood vessels requires the development of a conformal polymeric scaffold that exhibits vasoactive properties and improved permeability, as well as providing a surface for endothelial cell adhesion. Additionally, the outer layer of the artificial blood vessels must respond positively to fibroblast cells, as this region must interact with the surrounding connective tissue. The perfect small-diameter, tissue-engineered vascular grafts are designed to avoid the formation of blood clots within the vessel.

They are apt for treating high blood pressure and are harmonious with the structure of native blood vessels. However, the journey towards creating artificial blood vessels has its hurdles. These include inconsistencies in size or caliber, mechanical and biochemical properties that fall short compared to native vessels, and a distinct ultrastructural organization. The impact of these limitations is contingent on the specific environment and function of the artificial blood vessels. Researchers have explored using biodegradable synthetic polymers, natural polymers, and decellularized xenografts to overcome these challenges[103]. PCL, a synthetic biodegradable polymer, stands out due to its slow degradation rate, which facilitates sufficient tissue regeneration, superior mechanical properties, and a patency rate that endures for several months[104-106].

More recently, functional artificial blood vessels have been generated in vitro using biodegradable materials as scaffolds to facilitate the seeding, growth, and matrix production of vascular smooth muscle cells and endothelial cells through various manufacturing processes. Electrospinning, a technique that utilizes solutions of multiple polymers, has emerged as a popular method among various approaches for creating nanofiber scaffolds. This method effectively addresses the shortcomings associated with both synthetic and natural polymers. Furthermore, it offers enhanced biocompatibility along with superior physical and chemical properties.

In 2005, Vaz et al. were among the first to develop bilayer scaffolds for blood vessel applications; the exterior layer is made entirely of poly-lactic acid, a biodegradable thermoplastic derived from renewable resources. On the other hand, the interior layer is constructed solely from PCL, a synthetic biodegradable polymer known for its slow degradation rate and excellent mechanical properties[107]. However, separating these scaffolds' inner and outer layers resulted in poor mechanical properties. To address this issue, Nguyen et al. developed artificial blood vessels of different diameters in 2012 using multi-layered scaffolds composed of PCL -gelatin as the inner layer, poly(lactic-co-glycolic acid)-gelatin as the intermediate layer, and poly(lactic-co-glycolic acid)-CTS as the outer layer, using a double ejection electrospinning system[108]. These engineered artificial blood vessels exhibited flexibility, high tensile strength, resistance to intermediate pressure, and biocompatibility, with the ability to promote cell growth and proliferation for both fibroblast and endothelial cells. These results were confirmed by other

groups[109-111], and this multilayer approach was later used to generate multilayer grafts made from heterogeneous materials and structures, including a thin, dense, nanofibrous core composed of PCL and a thick, porous, hydrogel sleeve composed of Genipin crosslinked collagen-CTS **(Figure 5A)**. These grafts could sustain physiological conditions and promote cellular activities **(Figure 5B)**[112].

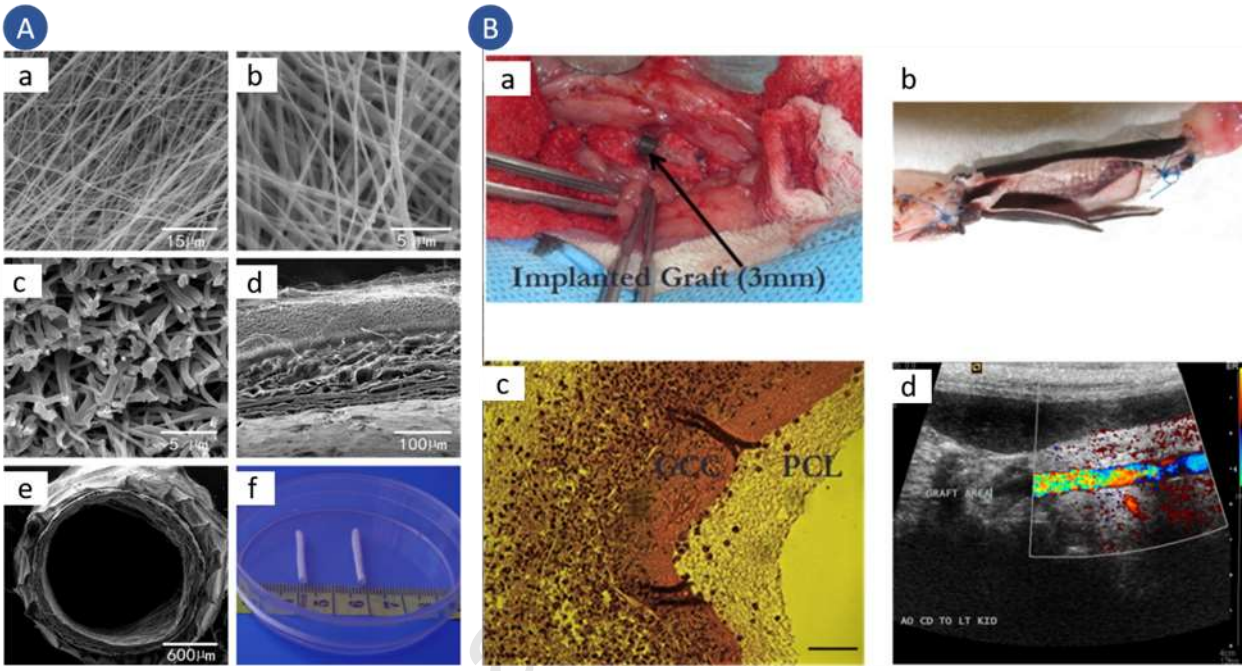

Figure 5: A) Structure characterization of electrospun PCL hybrid vascular grafts. **(a, b)** SEM images of nano-PCL fibers and **(c)** cross-section of nano-PCL fibers. **(d, e)** SEM images of a cross-section of HTEV grafts. **(f)** Digital optical image of PCL/DRA hybrid vascular grafts[113]. **B)** Biocompatibility evaluation of vascular grafts in vivo with a rabbit model. **(a)** A 3-mm-diameter multilayer vascular graft replaced the abdominal aorta of a rabbit with anastomosis covered with medical-use gauze; **(b)** the open-lumen view of an explanted multilayer vascular graft with neighboring arteries, showing no thrombosis or occlusion in the graft lumen; **(c)** optical image of the histological cross-sectional slice of an explanted graft stained with hematoxylin and eosin, showing the migration of cells from surrounding tissues mainly into the GCC layer rather than the PCL layer, scale bar:100 lm; **(d)** ultrasonic image showing blood reperfusion through the graft and the lumen without any thrombosis or stenosis[114].

In 2015, Agrawal et al. produced a highly aligned melt-spun PCL fiber scaffold that allowed for the aligned attachment of fibroblasts and vascular smooth muscle cells while preserving the contractile α-smooth muscle actin-expressing phenotype of the vascular smooth muscle cells. This technique is also applied to cell alignment on a prototype synthetic PCL vascular conduit[115]. These findings demonstrate the potential of using advanced fabrication techniques to create complex scaffold architectures for tissue engineering applications. In 2017, Gong and colleagues devised a hybrid small-diameter vascular graft by electrospinning PCL onto heparin-coated

decellularized matrices, demonstrating favorable biocompatibility and mechanical properties [116]. The following year, Ran and associates constructed a bilayer tissue-engineered vascular graft comprising a decellularized porcine coronary artery and electrospun PCL /gelatin fibers. Four weeks post-implantation in rats, the authors observed the development of an endothelial-like cell monolayer on the internal surface and the emergence of a dense middle layer composed of vascular smooth muscle cells. Ultimately, the regenerated vessels exhibited mechanical properties comparable to the rat abdominal aorta[117]. In a similar vein, the PCL /gelatin and heparin-loaded vascular graft has been reported as an efficacious biomaterial candidate for the fabrication of artificial small-diameter vascular grafts [118]. Most recently, a PCL-based vascular graft incorporating vascular endothelial growth factor was implanted in rats for 3 months and demonstrated favorable endothelialization and patency, elevated cellularity in the central region of all vascular grafts, and a properly formed adventitial surface[119].

While autologous revascularization remains the preferred approach in the treatment of cardiovascular disease, particularly in small-diameter vessel bypass procedures, due to the limitations of existing synthetic grafts, ongoing interdisciplinary research and rapidly advancing additive manufacturing technologies combined with regenerative medicine techniques are progressively revolutionizing the clinical management of these diseases. Through the development of biologically functional tissue-engineered constructs, including PCL, the pressing need for improved treatment options in the vascular field should be addressed through the biofabrication of the next generation of tissue-engineered vascular grafts.

3.6. Muscle

Tissue engineering has recently made significant strides, providing potential therapeutic options for a broad spectrum of disorders[120]. The musculoskeletal system, encompassing bones, tendons/ligaments, and muscles, is a primary focus of tissue engineering efforts[121]. Scaffolds are integral to the success of musculoskeletal tissue engineering, as they must support cells and facilitate neo-tissue formation at target sites. For skeletal muscle specifically, the tissue engineering scaffold must possess the capacity to endure inherent tensile forces, minimize scar formation, and furnish an optimal microenvironment for cell renewal, growth, and proliferation. Moreover, the polymer scaffold’s degradation and elimination cycle must align with the physiological muscle remodeling period.

Biomaterials with varying properties are prepared using diverse manufacturing methods based on the desired properties for different target tissues to reconstruct the musculoskeletal system. Electrospinning has garnered significant interest in producing large volumes of nonwoven fabric fibers at the nanoscale and microscopic scale, continuously, with high porosity, extensive surface area contact, and adjustable mechanical properties[122]. Electrospun membranes can replicate the natural extracellular matrix of various tissues, making them ideal for biomedical applications such as tissue engineering and regenerative medicine[123]. Flexible polymer membranes produced via electrospinning are well-suited for muscle injury recovery due to their cytocompatibility, biodegradability, and exceptional mechanical properties. Their extracellular matrix-mimicking structure enhances cell attachment to the membrane and furnishes an improved microenvironment for cell growth[124]. Numerous studies have reported the utilization of biodegradable biomaterials such as PCL, poly L-lactic acid, polyglycolic acid, and poly L-lactic acid/polyglycolic acid copolymer as scaffolding for musculoskeletal tissue engineering[125]. PCL, in particular, exhibits favorable biocompatibility and low immunogenicity, with the added benefit of slow degradation into non-toxic metabolic products[126]. The degradation time of PCL fibers exceeds 2 years, aligning with metabolism and muscle regeneration timeframes[127]. Muscle stem cells are attracted to the injured area during muscle regeneration, differentiating into muscle cells and ultimately ensuring complete tissue reformation[128].

In addition to biocompatibility, physiological compatibility between cells and the biomaterial surface is crucial for supporting skeletal muscle tissue reconstruction in the injured region[129]. Research has investigated the impact of fiber diameter on cell adhesion and proliferation, revealing that smaller-diameter fibrous membranes generally facilitate improved cell migration, propagation, signaling, and replication[130]. Consequently, electrospun membranes' fiber diameter and surface affinity play a significant role in tissue engineering.

In 2017, Liu et al. fabricated PCL fibrous membranes with varying fiber diameters (2 μm and 10 μm) via electrospinning to create a scaffold that is resistant to tensile force, minimizes scar formation, and provides an optimal microenvironment for cell growth and proliferation[131]. These membranes were subsequently coated with poly-norepinephrine via self-polymerization, a catecholamine molecule that regulates muscle contraction. The authors reported that these

norepinephrine-coated PCL scaffolds positively impacted muscle cell adhesion and proliferation, resulting in improved tissue restoration[131].

In 2020, Navaei et al. designed and fabricated a 3D-printed porous scaffold composed of PCL and gelatin, intended for use as scaffold patches for diaphragm muscle repair and regeneration[132]. These scaffolds exhibited exceptional mechanical tensile strength and in vivo biocompatibility **(Figure 6A)**, demonstrating the potential of these composite PCL and gelatin scaffolds for reconstructing striated skeletal muscles of the diaphragm[132].

In 2021, Perez-Puyana et al. sought to enhance the characteristics of PCL scaffolds by incorporating elastin, resulting in improved cell proliferation, biocompatibility, and mechanical properties more closely resembling those of muscle tissue[133]. Their findings further indicate that the inclusion of elastin in PCL scaffolds produces uniquely aligned scaffolds that are more hydrophilic and have smaller fiber sizes[133].

In 2022, Aparicio-Collado et al. integrated reduced graphene oxide into PCL scaffolds to imbue them with unique electrical properties[134]. These features collectively enhance the biocompatibility of the scaffolds, facilitating improved tissue interconnection and integration, particularly in skeletal muscle tissue engineering.

3.7. Cardiac

Charitidis et al. [135] synthesized a CTS-graft-PCL copolymer and utilized it for myocardium regeneration by culturing Wharton's jelly mesenchymal stem cells (WJ-MSCs) on 3D CTS-g-PCL scaffolds and differentiating them into cardiac cells under cardiogenic induction using oxytocin. The graft copolymer exhibited Young's modulus comparable to that of soft tissues, supported the growth and proliferation of WJ-MSCs, and demonstrated potential for use in myocardium tissue engineering.

Repanas et al. fabricated flexible PCL-CTS fibrous scaffolds through electrospinning and combining nano- and micro-fibers. Preliminary fiber characterizations yielded suitable mechanical properties, while biocompatibility studies indicated that the scaffolds provided an appropriate cell environment for cardiovascular tissue engineering[136].

MEI et al. produced PCL porous scaffolds using a particle-leaching technique and subsequently coated the PCL scaffolds with CTS by immersing them in CTS solutions of varying

concentrations. Cell culture studies revealed improved fibroblast cell attachment to the PCL scaffolds, and CTS enhanced the biocompatibility of the PCL scaffolds commonly employed in cardiovascular tissue engineering. This study demonstrated the advantages of CTS-modified PCL scaffolds for heart valve tissue engineering **(Figure 6B)**[137].

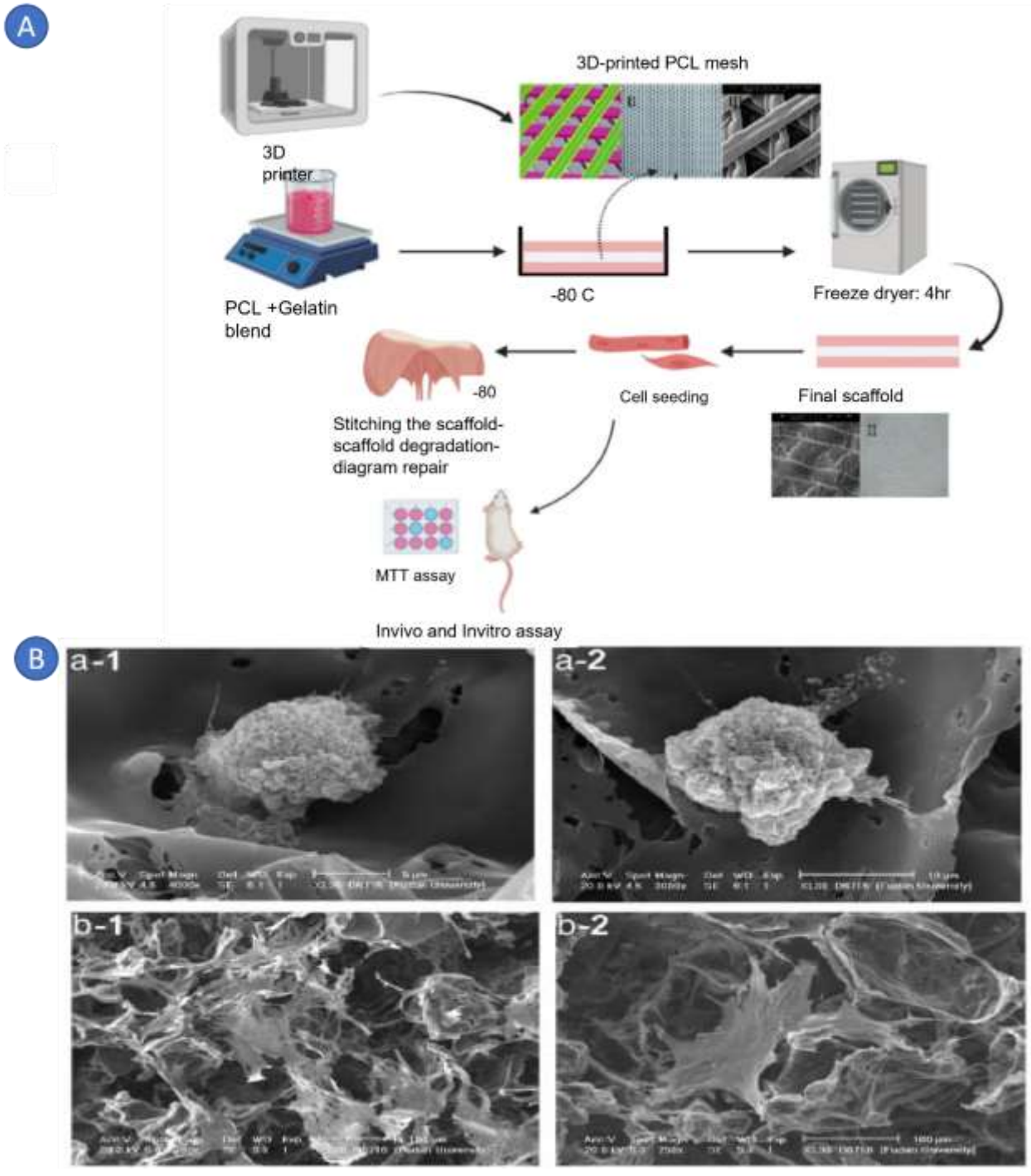

Figure 6: A) Diagram illustrating the procedure for creating and managing the fabrication process [138]. **B)** SEM images of fibroblasts after a different number of days' culture on the scaffolds. Cells attached on the surface of PCL

(a-1) and CTS-modified scaffold CTS/PCL **(a-2)** for 1 day; cells proliferated on the surfaces of the PCL scaffold **(b-1)** and CTS-PCL scaffold **(b-2)** for 3 days[137].

3.8. Eye

Corneal endothelial cells (CECs) have restricted proliferation abilities in vivo, which makes them challenging to repair. Cultured CECs can be seeded successfully as transplantation grafts on natural tissue or synthetic polymeric materials in vitro. Research is being conducted on the best substratum for CEC growth [139].

3.8.1. Corneal

The cornea, a transparent structure located at the anterior portion of the eye, plays a crucial role in vision by transmitting and refracting light. Comprised of multiple layers, including the epithelium, stroma, and endothelium, the cornea's unique anatomical structure facilitates its function[61].

However, this same structure presents challenges for the delivery of therapeutics. Clinically approved formulations, such as eye drops and ointments, exhibit low bioavailability following topical administration due to the presence of anatomical and physiological barriers that prevent the entry of foreign compounds[140].

In recent decades, significant efforts have been made to develop efficient topical formulations that enhance the bioavailability of ophthalmic drugs. One approach involves using biodegradable and biocompatible polymeric hydrogels to prolong the residence time of the drug in contact with corneal tissue. Another strategy employs nanomedicine and nanotechnology to facilitate intimate interactions between drug molecules and specific ocular tissues[140].

CTS and PCL are two biodegradable biomaterials that have received approval from the Food and Drug Administration and offer considerable advantages. These materials can be blended harmoniously without the need for complex chemical modifications **(Figure 7A)**[141].

3.8.2. Retinal

The use of biodegradable scaffolds for delivering retinal progenitor cells (RPCs) represents a promising therapy for restoring injured or diseased retinal tissue[142]. Biocompatible polymer scaffolds have shown potential as carriers for RPCs in cell replacement therapy aimed at repairing damaged or diseased retinas[143]. Critical factors in the success of retinal tissue engineering procedures include biocompatibility, non-toxicity, the ability to provide appropriate signaling, and suitable physical properties such as modulus of elasticity. Recent advances in the production of polymers such as PGA, PLLA, PDLLA, HA, PCL, and CTS have led to the development of polymer scaffolds for use in the retina **(Figure 7B)**[144].

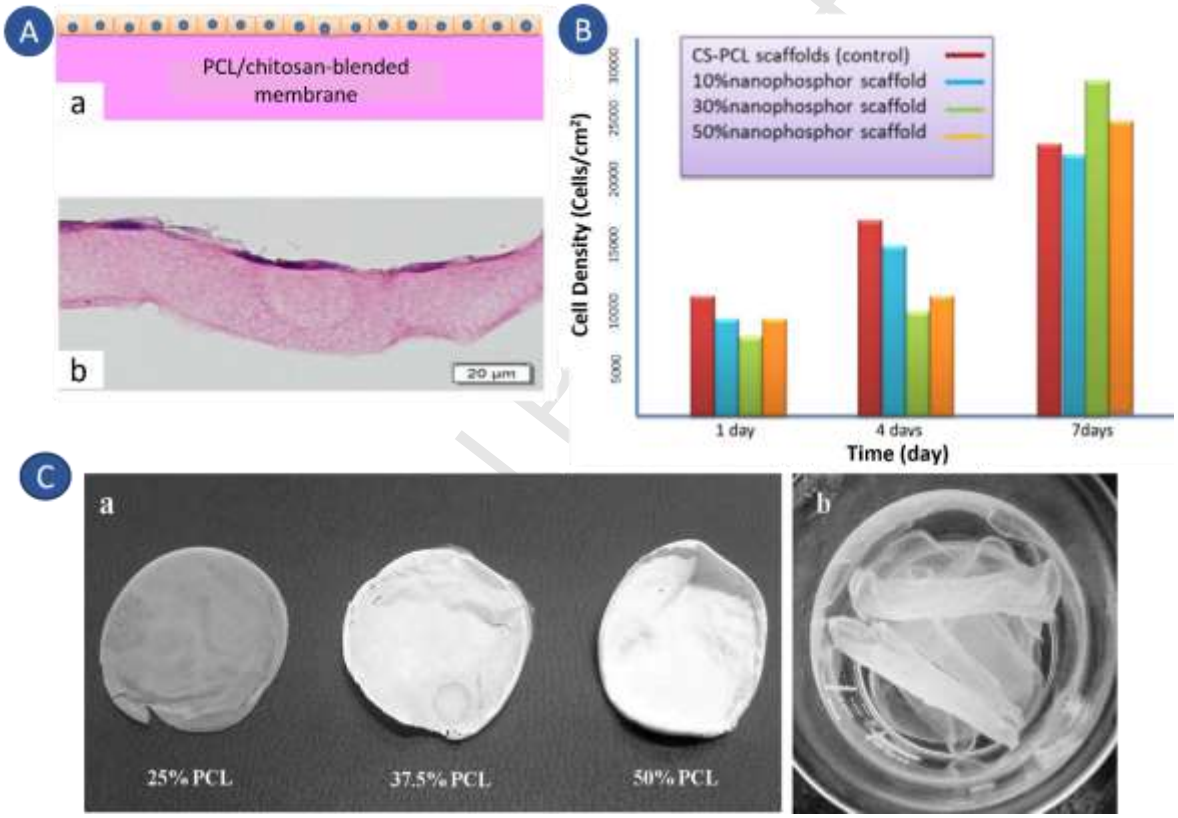

Figure 7: A) Fabrication of a Bioengineered Corneal Endothelial Cell Sheet Using CTS/ PCL Blend Membranes[145]. **B)** Proliferation of the mRPCs on CTS-PCL scaffolds (control) and SrAl2O4:Eu2+, Dy3+/ CTS-PCL electrospun three scaffolds after culturing for 1, 4and 7 days[146]. **C)** Macroscopic photos show that the **(a)** apparent transparency of the dried composite membranes reduced as the PCL content increased. **(b)** Immersing CTS/PCL 50/25 membranes in PBS resulted in a significant increase in transparency and flexibility compared to the membranes that were dried[147].

CTS and PCL are biodegradable biomaterials that have received approval from the Food and Drug Administration (FDA) and offer numerous advantages[148]. Corneal scaffolds can be constructed from both natural and synthetic polymers, with natural polymers such as gelatin,

collagen, silk, hyaluronic acid, cellulose, and CTS being widely used in ocular tissue engineering[61].

CTS, a linear polysaccharide, possesses a wide array of applications within the field of tissue engineering owing to its abundant presence, diverse physicochemical characteristics, compatibility with biological systems, and ability to degrade over time. However, its insolubility in organic solvents and extreme brittleness have hindered fundamental research and application. An alternative is the use of PCL, a semicrystalline biodegradable polyester[144].

CTS is an ideal substrate for cell attachment and growth due to its aqueous solubility, biocompatibility, biodegradability, antibacterial and antifungal activity, and mucoadhesive and hemostatic properties. However, despite the ease with which CTS films can be produced via solvent casting and subsequent solvent evaporation, the films exhibit poor mechanical properties and are prone to degradation. This lack of mechanical strength is a fundamental limitation of CTS and other natural biomaterials, restricting their use in scaffold construction. One approach to overcoming this limitation is the incorporation of nanoparticles into scaffolds[149].

PCL is a synthetic polymer that has received approval from the FDA and is widely used in regenerative medicine. Due to its ease of processing and responsiveness to surface modifications, PCL is an attractive candidate for biomedical applications such as ocular tissue engineering and drug delivery. However, the inclusion of PCL in scaffolds can compromise their structural integrity. By combining polymers, it is possible to create a range of composite scaffolds with desirable biological and biochemical properties, potentially enhancing corneal regeneration **(Figure 7C)**[61].

CTS, a fully or partially deacetylated chitin, has been utilized in various biomedical applications due to its excellent biocompatibility, low toxicity, and antimicrobial properties. These applications include drug delivery systems, wound dressings, and nerve regeneration agents. However, CTS's potential has been hindered by its low electrospinnability, insolubility in common organic solvents, and brittleness. PCL, a semicrystalline biodegradable polyester, has been approved by the US FDA for several clinical applications in humans due to its high biocompatibility, mechanical properties, and lack of toxicity. It is also commonly used as a scaffold material in tissue engineering. However, PCL's disadvantages, such as its high hydrophobicity, slow degradation kinetics, and lack of bioactive activities, have limited its use as a tissue engineering substrate. Combining the bioactive properties of CTS with the superior

mechanical properties of PCL to create a novel biohybrid material should result in improved biological, mechanical, and degradation properties compared to the individual components. CTS-PCL nanofibrous scaffolds have been produced using solvent solutions such as trifluoroacetic acid and hexafluoro-2-propanol[150].

However, it should be noted that these solvents are relatively expensive compared to traditional solvent systems, and their nature may result in accelerated polymer degradation. In this study, a CTS-PCL copolymer was synthesized by grafting -caprolactone oligomers onto the hydroxyl groups of CTS via ring-opening polymerization and then blended with PCL to create a 3-dimensional CTS-PCL/PCL scaffold. The electrospinning of blend solutions in a common solvent system produced the CTS-PCL/PCL scaffolds, which were expected to be easy to fabricate. Furthermore, the grafting modification of CTS was anticipated to enhance interfacial adhesion with the PCL fiber matrix. The properties of the CTS-PCL/PCL scaffolds, including wettability, surface topography, and porosity, were investigated[151].

When CTS and PCL were successfully hybridized into blended membranes, CECs proliferated, exhibited normal morphology and retained their physiological characteristics[139].

CTS is a biodegradable biomaterial composed of a linear polysaccharide with a variable number of randomly distributed N-acetylglucosamine groups. It is derived from deacetylated chitin, Earth's second most abundant polymer. Like glycosaminoglycan in the extracellular matrix (ECM), CTS offers numerous advantages, including biocompatibility, biodegradability, non-antigenicity, wound-healing properties, and low cost. It also promotes the formation of ECM. However, its current application in tissue engineering is limited due to its low strength and limited understanding of cellular interactions. Various approaches have been employed to overcome these limitations, including graft polymerization and blending. Interestingly, polymer blends have improved biological, mechanical, and degradation properties compared to separate culturing substrates. PCL has long been an implantable material due to its excellent tensile properties as a biocompatible polyester. According to previous research, PCL also enhances cell attachment. Cells regulate gene expression and produce collagen on CTS-PCL blends by altering cell shape. As a result, the current study focuses on the behavior of CECs on CS and PCL blends based on the distinct adhesion effects on CTS and PCL[152].

Despite its great potential, CTS has several fundamental limitations restricting its use in tissue engineering. These include low electrospinnability, insolubility in common organic solvents, and

high brittleness[153]. However, CTS can be combined with other biomaterials, such as PCL, to create blended materials that retain unique advantages while overcoming these limitations. The blending process can be achieved simply without complex solvents or chemical modifications. In this study, we investigated the underlying mechanisms and developed a potential alternative using CTS-PCL blends to produce CEC sheets with well-preserved CEC properties[154].

3.9. Lung

The lungs serve as the primary organ for gaseous exchange, facilitating respiration. The human respiratory system comprises two distinct zones: the conducting and respiratory zones. The conducting zone provides a passage for airflow and conditions incoming air, while gas exchange occurs in the respiratory zone. The respiratory zone begins at the terminal bronchioles and extends to the alveoli, sac-like structures distributed throughout both lungs. The basement membrane of the alveoli forms a barrier with capillaries, allowing for gas diffusion. During inhalation and exhalation, the volume of the lungs changes due to the action of the diaphragm and intercostal muscles. However, in cases of pneumonia, sepsis, or acute respiratory distress syndrome, increased permeability edema can cause fluid to flood the alveoli, significantly reducing the lungs' capacity for gaseous exchange and leading to high mortality rates. Organ transplantation is often necessary in such cases, but a shortage of donors presents a significant challenge. As a result, attention has shifted towards alternative treatment approaches, such as tissue engineering and microfluidics[155].

Engineering lung tissue necessitates transplanting patient-derived cells onto meticulously designed scaffolds, augmenting cellular adherence, metabolic activity, and biocompatibility. The selection of an appropriate material for synthesizing a lung scaffold is contingent upon the material's mechanical properties, as the cells within lung tissue are subjected to continuous stress. The structural and biochemical characteristics of lung tissue can be attributed to the presence of an array of proteins, including collagen, elastin, and fibronectin, which provide support to the cells[156].

The advent of PCL scaffolds has opened many opportunities for creating novel materials with robust mechanical properties. PCL scaffolds have been demonstrated to possess steeper stress-strain curves and superior biodegradability[157]. Incorporating CTS into PCL enhances the wettability of the resulting scaffold. Since the mechanical properties of a scaffold are correlated

with its wettability, PCL-CTS blend scaffolds exhibit a combination of rigidity and elasticity. Numerous studies have employed PCL-CTS scaffolds in lung tissue engineering, evaluating the physical, mechanical, and biodegradability properties of the scaffolds, the viscous characteristics of the blends, and their associated biocompatibility.

3.9.1. 3D bioprinting approach

In tissue engineering, researchers employ various 3D bioprinting techniques, selecting an appropriate method based on the printing quality and resolution of the print[158]. Rezaei et al. utilized a surface response methodology and central composite design to determine the optimal proportions of PCL and CTS[157]. The concentrations of PCL and CTS in the scaffold varied within the range of 1-4% following the experimental design strategy, and the scaffolds were printed using a 3D bio-plotter. Subsequent rheometric measurements were conducted to characterize the viscous behavior of the scaffolds, with those exhibiting viscosities less than 1000 cP demonstrating poor printability and thus being excluded from further analysis. Scaffolds with viscosities within the range of 1000-1340 cP exhibited superior printability, and the researchers derived an equation based on multiple trials to identify an optimal blend, utilizing two parameters: A (PCL concentration) and B (CTS concentration).

$$P = 2 + 0.83*A + 0.17*B + 4.5e^{-16}*AB + 0.5*A^2 - 0.5*B^2$$

The above equation considers the first-order effects (A, B), interaction effects (AB), and second-order effects (A^2, B^2). Rezaei et al. showed that the above equation was suitable for determining printability (P), as evidenced by an R^2 value of 0.9.

Furthermore, scaffolds containing a low concentration of PCL exhibited the highest degree of swellability. As swellability is associated with the ability of cells within a scaffold to exchange nutrients, blends with a low PCL content facilitate enhanced nutrient exchange. The authors also observed that stiffer scaffolds were achieved by reducing the CTS-PCL ratio, with scaffolds possessing a 2:1 or 3:1 CTS-PCL ratio exhibiting superior elongation behavior compared to those with a 4:1 ratio. These scaffolds were selected to mimic lung expansion through tissue engineering **(Figure 8A).** Cell attachment increased with PCL concentration, as seen in the 48 h post-cell culture. Moreover, the live-dead assays showed the CTS-PCL scaffolds with low toxicity **(Figure 8B)**[157].

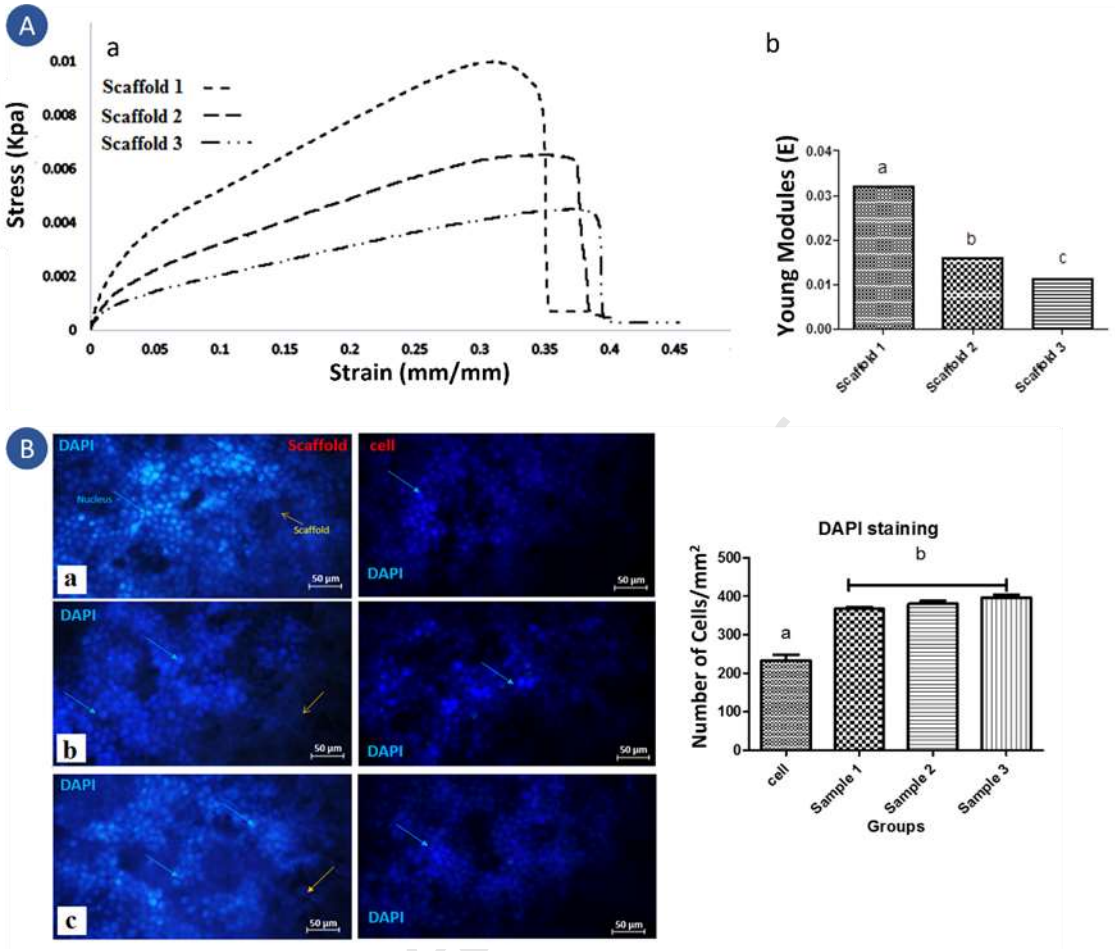

Figure 8: A) Stress-strain diagram for **(a)** Scaffold 1 (2:1), Scaffold 2 (3:1), Scaffold 3 (4:1), and **(b)** Young modulus for the scaffolds. **B)** Fluorescence images of DAPI-stained MRC-5 cells on **(a)** Scaffold 1, **(b)** Scaffold 2, and **(c)** Scaffold 3.

3.9.2. Electrospinning approach

Mahoney et al. employed electrospinning to prepare composite nanofibers by mixing depolymerized CTS with PCL. CTS was depolymerized through oxidative degradation using sodium nitrate, and the resulting scaffold was subjected to mechanical testing using a tensile-test machine[159]. Solutions with higher PCL-CTS ratios exhibited superior electrospinnability, producing smooth fibers with minimal beads. When the PCL-CTS ratio was 7:3, the nanofibers were stable and completely devoid of beads. Furthermore, an increase in the CTS content resulted in a decrease in fiber diameter. In contrast, an increased PCL ratio led to enhanced elasticity, and a reduced ratio increased scaffold stiffness. The Young's modulus of the PCL-CTS nanofibers was in agreement with that of sheep trachea (10.6 ± 1.8 MPa). When incubated with PTBE cells, the scaffolds demonstrated suitable cell attachment, and the results of both the

cell attachment and mechanical properties indicated that the PCL-CTS scaffolds were ideal for supporting the growth of lung epithelial cells and tracheal regeneration **(Figure 9A).**

In a related study, Leary et al. developed a PCL-CTS scaffold impregnated with retinoic acid, a signaling molecule[6]. The nanofibers were fabricated using the electrospinning method, and like the findings of Mahoney et al., the authors observed that an increase in PCL concentration resulted in larger fiber diameters. When the PCL concentration was 5% or 10%, combined with 0.5% CTS, homogenous nanofibers were produced. The scaffolds were biocompatible with Calu3 epithelial cells at these concentrations, as demonstrated by a 14-day viability study. Furthermore, the expression of mucin, a phenotypic marker of the tracheobronchial tree, increased 7-fold when the scaffold was loaded with 10 ug/mg of retinoic acid **(Figure 9B)**. Overall, Leary et al. demonstrated the suitability of electrospinning as a method for fabricating biocompatible scaffolds for tracheal replacement[6, 159].

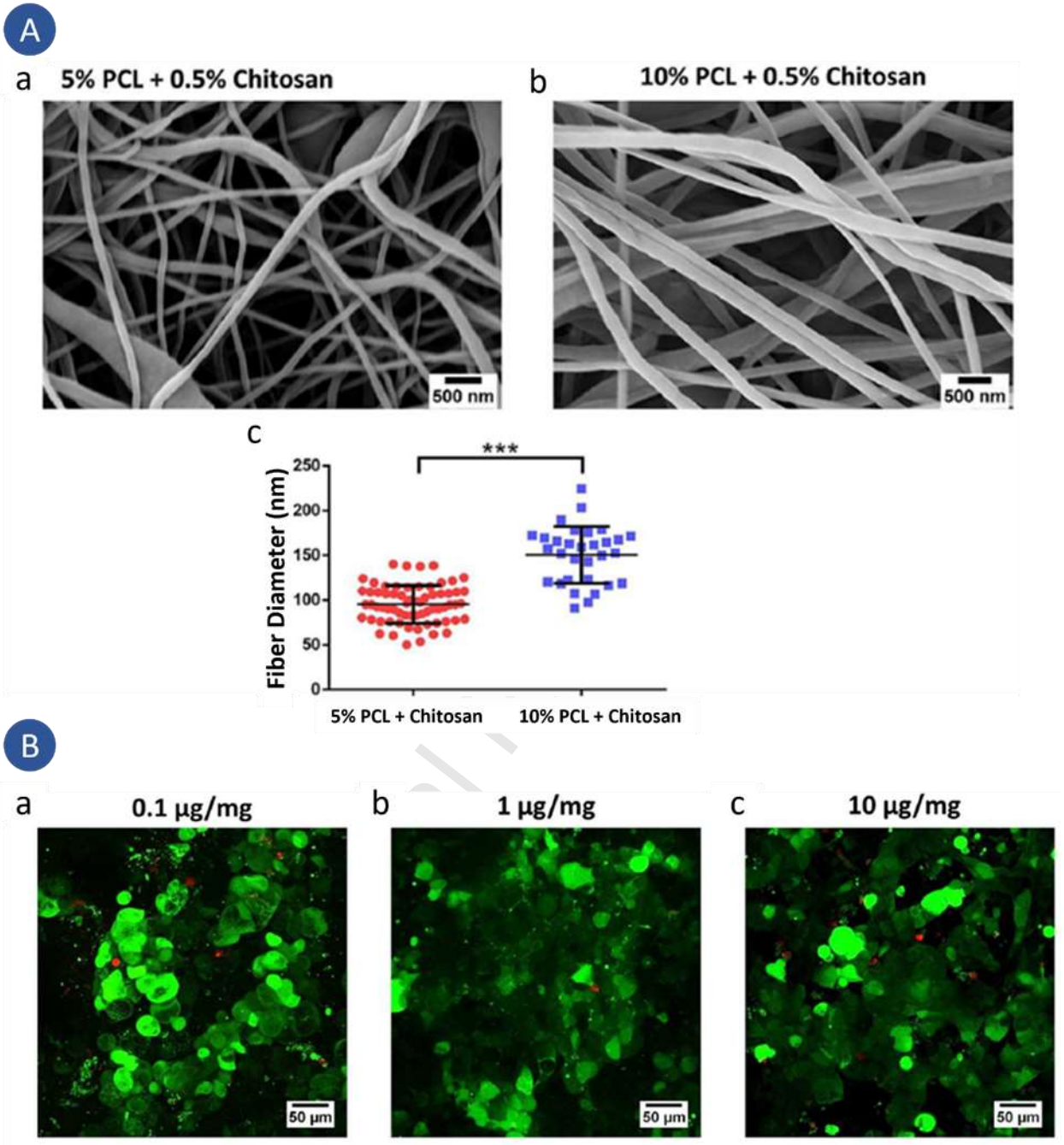

Figure 9: A) Fabrication of PCL-CTS scaffolds showing **(a)** 5%/0.5%, **(b)** 10%/0.5%, and **(c)** Mean diameter of electrospunfibers. **B)** Fluorescent images showing biocompatibility of retinoic acid-loaded 10%PCL-0.5% CTS with retinoic acid concentrations of **(a)** 0.1 ug/mg, **(b)** 1 ug/mg, and **(c)** 10 ug/mg.

3.9.3. Phase separation approach

In 2005, Mei and colleagues reported fabricating a PCL-CTS scaffold using the particle leaching method, which involves phase separation[137]. This process entails the removal of solute from an

admixture with a solid by contacting it with a solvent. The PCL scaffold was submerged in various concentrations of CTS, and the resulting scaffold was incubated with fibroblasts. Lung fibroblasts play a crucial role in maintaining the integrity of the alveolar structure by proliferating and repairing injured areas. Within the lung interstitium, fibroblasts are responsible for ECM production; thus, the fabrication of a scaffold suitable for incubating fibroblasts can aid in repairing damaged alveoli. Seven days post-incubation with fibroblasts, the cell population increased, and the cells appeared elongated and firmly attached to the scaffold. Furthermore, an MTT assay revealed that the scaffold facilitated improved attachment.

3.10. Liver

The liver, the largest internal organ in the human body, is responsible to execute over 500 distinct functions to maintain homeostasis[160]. Comprising 2-5% of the total body weight, the liver's ability to regulate glucose homeostasis, blood dynamics, lipid and lipoprotein synthesis and distribution, serum protein production, amino acid synthesis, vitamin and mineral storage, drug and toxin metabolism, coagulation factors, growth factors, foreign component inactivation, and antigen presentation makes it one of the most effective organs in the body[161].

Liver damage can result from a variety of causes, including physical injury, alcohol abuse, drug or toxin-related injury, cancer, and various forms of hepatitis. Depending on the cause of injury, liver damage can manifest as chronic liver disease due to metabolic dysfunction, acute liver failure (ALF) or chronic liver failure (CLF)[162].

Liver disease, despite being largely preventable, accounts for nearly 2 million deaths worldwide each year[163]. Once diagnosed, treatment options for liver disease are limited, leading to an increased need for liver transplants, making it the second most common solid organ transplantation **(Figure 10B)**[164]. The liver's unique ability to regenerate and fully restore its mass and function has led to the use of tissue engineering methods to address the issue of liver transplants. Liver tissue engineering requires an ideal ECM for hepatocyte culture to retain a high level of liver-specific functions. The ECM is the interactive base in which cells adhere, grow, migrate, differentiate, and interact with other cells. Hepatocytes are polarized cells; this polarity must be maintained for optimal cell performance. In vivo, liver ECM effectively maintains polarity and cell function by presenting a gradient of solid and soluble factors. As such, a suitable ECM or scaffold is necessary to keep the hepatocyte phenotype[165].

In the realm of biocompatible polymers, both synthetic and natural, PCL and CTS have emerged as practical choices for the fabrication of scaffolds. These materials possess desirable properties such as biocompatibility, processability, and controlled biodegradability[166]. PCL, a hydrophobic polymer, presents challenges for cell seeding. However, Huang et al. demonstrated its potential for culturing hepatic cells[167]. CTS, a hydrophilic charged polymer, has been widely used as a matrix for hepatocyte culture due to its similarity to glycosaminoglycan. Various forms of CTS scaffolds, including composites, membranes, hydrogels, foams, microcarriers, and micro- and nanofibers, have been employed to support hepatocytes in vitro[168, 169]. Chemical modification of CTS's functional groups can introduce new properties. For example, galactosylated CTS (GCS), obtained by introducing galactose moieties into CTS, is favorable for hepatocyte growth in the form of microspheres[170, 171]. Yuan and colleagues sought to improve the bioartificial liver system by modifying PCL with GCS. GC was synthesized by coupling LA with CTS using EDC and NHS as catalysts. The PCL scaffold was prepared using a gelatin particle leaching method in NaOH solution, introducing COOH groups[172, 173]. The presence of carboxyl groups stabilized the CTS on the PCL scaffold, resulting in a significant increase in mechanical strength. Another study showed that the mechanical properties of PCL/GC were higher than those of PCL-CTS, and electrospinning of PCL-GC resulted in even higher mechanical properties. GCS increased the diameter of PCL nanofibers from 63nm to 83nm, increasing the strength of the scaffold from 4.18 to 6.15 MPa. Contact angle tests showed that GCS reduced the contact angle, increasing the hydrophobicity and solubility of CTS, making the electrospinning process easier and resulting in nanofiber diameters up to 97nm[174].

Yuan et al. demonstrated that immobilization of GCS on a PCL scaffold resulted in impressive viability, desired 3D morphology, and higher albumin secretion levels in human hepatoma cell line HepG2 cells in vitro. Ghahremanzadeh and colleagues also showed that HepG2 cell viability on PCL/GC scaffolds was improved due to the availability of galactose on the scaffold surface **(Figure 10A)**[174, 175]. Scaffolds play a crucial role in tissue engineering, and it is vital to investigate the factors contributing to an effective scaffold. Electrospinning has recently gained attention among the various methods for constructing scaffolds due to its remarkable features.

Semnani et al. created a nanofibrous scaffold for liver tissue engineering by electrospinning PCL and CTS. They used a novel collector to improve orientation and pore size for cell infiltration, as

pore size, porosity, and fiber diameter are crucial factors in achieving an effective scaffold. Among the nanofibers fabricated under various conditions, PCL-CTS with a collector speed of 90 rpm and a collector wire angle of 40 degrees produced nanofibers with a diameter of 243±32 nm, 79% porosity, and a pore size of 12±5 μm. These porosity and pore size values were suitable for infiltration and material exchange by mouse liver epithelial cells (Hepa 1-6). Cell culture and MTT results demonstrated the non-toxicity and compatibility of the scaffold[1].

3.11. Kidney

The kidneys, two organs situated within the abdominal cavity, are responsible for regulating the urinary system. The nephron, the functional unit of the kidneys, performs many tasks, including urine production and elimination, as well as blood filtration. Given the critical role of the kidneys in maintaining human health, kidney diseases and chronic kidney disease (CKD) are medical conditions of significant clinical concern, particularly when organ function is severely impaired[176].

Hemodialysis (HD) is the primary treatment for patients with chronic CKD, effectively clearing small water-soluble uremic toxins. However, HD is less effective in clearing protein-bound uremic toxins (PBUTs)[177]. Xiong et al. developed a more efficient dialyzer, utilizing a sponge-like PCL-CTS porous monolith as a single-use absorbent for uremic toxin sorption [178]. The PCL-CTS sponge was created using a vapor-induced phase separation (VIPS) technique, which leverages water vapor to initiate the phase separation process and generate symmetrically distributed internal and external micro pores within the hydrophobic polymeric structure[179]. CTS was utilized as a functional composite at varying concentrations (wt%), while PCL served as a supporting material. Porous carbon was also integrated into the PCL-CTS sponge. This addition formed an absorbent matrix characterized by its multiple absorptive components. The primary function of this matrix is to facilitate the removal of uremic toxins. Notable among these toxins are Albumin-Bound Indoxyl Sulfate and creatinine. After 1 hour of single-pass perfusion, a maximum unit weight absorbability of 436 μg/g for albumin-bound indoxyl sulfate and 2865 μg/g for creatinine was achieved. The proposed PCL-CTS porous monolith has the potential to absorb uremic toxins, including PBUTs; this advancement paves the way for the rejuvenation of spent dialysate. It also fosters the creation of a novel dialysis treatment class that harmonizes with the environment. A prime example of such treatments is the wearable artificial kidney.

The global incidence of end-stage kidney disease (ESKD) continues to rise, with organ transplantation remaining the primary option for replacing the functionality of damaged kidneys [180]. However, transplantation is associated with numerous challenges, including rejection, loss of kidney function, or death within 5-10 years[181]. To address these limitations, innovative and alternative approaches based on nano- and biomaterials have been employed in the treatment and regeneration of renal tissue[182].

CTS has demonstrated intrinsic beneficial properties for the kidneys and has been tested for efficacy in patients undergoing long-term stable HD treatment with renal failure. Data showed significant reductions in serum urea and creatinine levels after 4 weeks of CTS ingestion, with no clinically problematic symptoms observed. These results suggest that CTS may be an effective treatment for renal failure patients, though the mechanism of its effect requires further investigation[183]. In another 12-week study, CTS (1450 mg/day) was shown to reduce serum cholesterol, increase mean serum hemoglobin, and reduce creatinine compared to a control group [32, 184].

CTS has also been tested for its stimulating effects on renal proximal tubule cells (RPTCs), responsible for glomerular filtration and maintaining water/electrolyte balance. Human RPTCs were supplemented with CTS for 150 days to evaluate their intrinsic effect as a substrate on cell function. Cells grown on CTS exhibited increased dome formation, higher Na(+) -K(+) ATPase expression, lower vimentin expression, and lower transepithelial electrical resistance compared to cells grown on a collagen substrate. These data indicate that human RPTCs grown on CTS exhibit better differentiation status and may be more functional, with improved active transportation for proximal tubule regeneration[185]. These results demonstrate the effectiveness of a natural biomaterial, such as CTS, in improving the clinical picture in cases of kidney disease. Indeed, CTS has emerged as a suitable biomaterial for scaffold design and cell carrier for proximal tubules and kidney tissue engineering[186, 187].

PCL, a synthetic biomaterial, has been tested both alone and in combination with other synthetic (polyethylene glycol), natural (collagen, CTS), or protein (laminin) materials for the development of hybrid scaffolds for the treatment of renal disease **(Figure 10 C)**[33, 188-190].

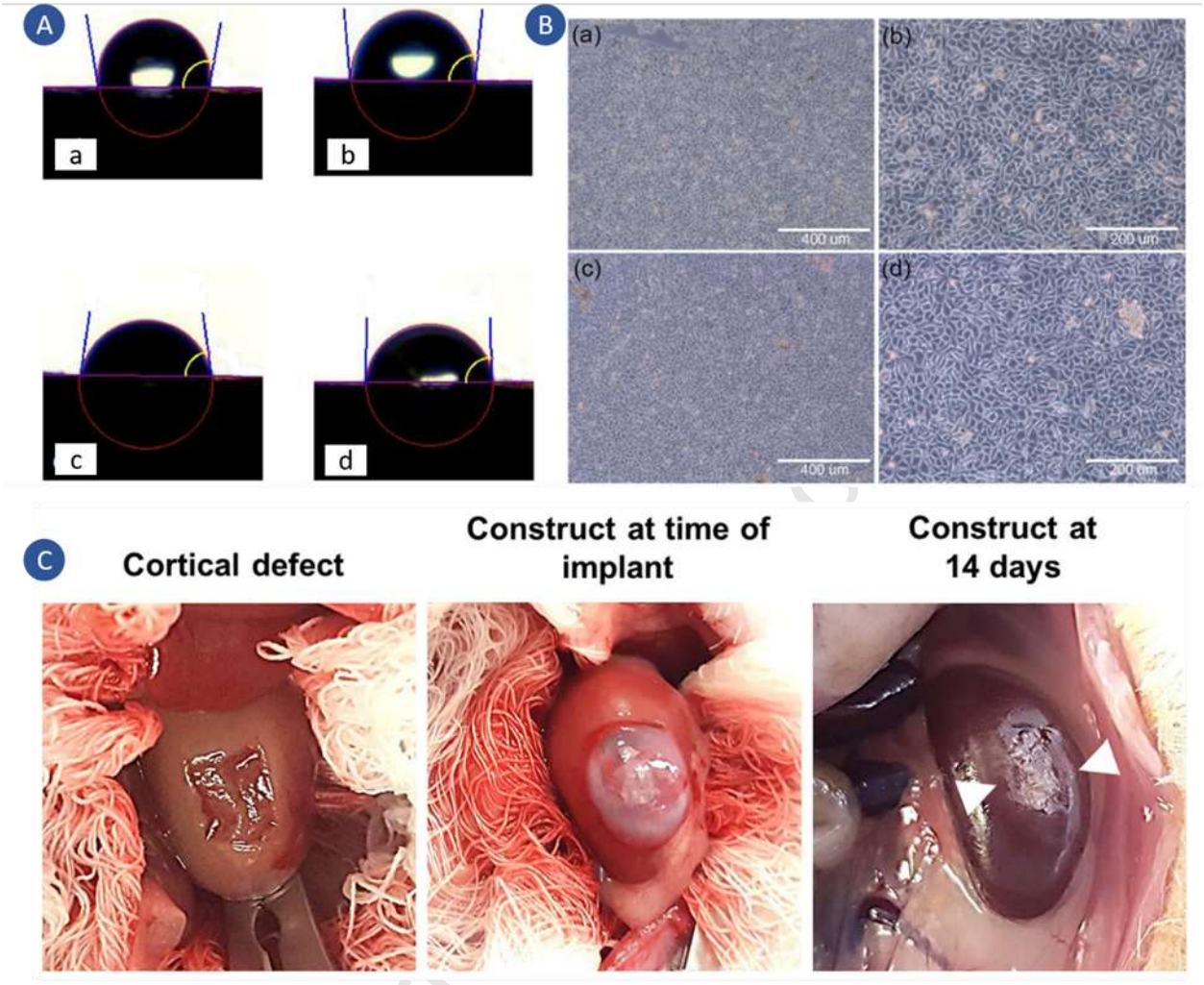

Figure 10: A) Water Contact Angle of Raw PCL/CTS nanofibers **(a)**, PCL/GC nanofibers **(b)**, Galactosylation after electrospinning of PCL/CTS nanofibers **(c)** and in-situ galactosylation of PCL/CTS nanofibers **(d)**, (n = 3)[175]. **B)** Microscopic images of each experimental group with 400 µm and 200 µm magnification: **(a,b)** PCL cell culture scaffold; **(c,d)** PCEC–PCL cell culture scaffolds[191]. **C)** Gross images from the renal implantation surgery. After clamping the renal vascular pedicle, a rectangular section of the cortex was removed. The construct was placed in the defect and secured with fibrin glue. At 14 days, the construct was still in place (white arrows)[33].

Simsek et al. utilized the electrospinning technique to produce PCL-CTS membranes composed of submicron fibers of varying size (200-550nm) and orientation (random and aligned) to evaluate their effect on epithelial Madine Darby Bovine Kidney (MDBK) cells[192]. Results indicated that fiber orientation had the greatest impact on cell morphology in contact with the PCL/CTS membranes. Epithelial cells exhibited a spindle-like morphology directed by aligned fibers, while less contact guidance was observed on random fibers. Additionally, PCL/CTS supplemented with collagen increased F-actin filament synthesis in MDBK cells. This study investigated the effect of surface topography on cellular behavior. It demonstrated that size,

chemical composition, and fiber orientation affected cell morphology, spreading, and F-actin synthesis to varying degrees. These data are important for achieving a fundamental understanding of complex cell-material interactions and advancing biomaterials applications[193].

3.12. Nerve

The nervous system is divided into the central nervous system (CNS) and the peripheral nervous system (PNS). The CNS comprises the brain, brainstem, cerebellum, and spinal cord, while the PNS consists of afferent sensory fibers and efferent motor fibers that project to striated skeletal muscle, innervating target tissues via the neuromuscular junction. The PNS can generally be considered a bridge connecting the body with its environment[194]. Peripheral nerve injury often results from tumor resection, reconstructive surgery, or trauma, with an average of 18 people per 100,000 suffering from intensive peripheral nerve injuries annually[195]. Due to the complexity and delicacy of the CNS, regeneration of the PNS is more feasible than that of the CNS. However, complete recovery of the PNS is not easily achieved, particularly in cases of severe nerve damage[196].

Methods for peripheral nerve regeneration focus on clinical, functional, and histological perspectives to enhance the nerve repair process. One of the fundamental challenges in peripheral nerve regeneration is bridging nerve gaps following injury. To address this issue, Akbari et al. designed PCL-CTS nanofibrous scaffolds using the electrospinning method in 2008, assessing their efficacy in vitro with rat Schwann cells for tissue engineering. Results indicated that adding CTS to PCL reduced the fiber diameter of PCL from 630 nm to 190 nm, an advantage for nanofibers. This combination also increased hydrophilicity, decreasing the contact angle of PCL from 108 to 30 degrees. Superior cell attachment and proliferation of Schwann cells on PCL-CTS were also observed, confirming PCL-CTS as a potential biocomposite material for effective nerve regeneration[197]. In 2011, Cooper et al. utilized aligned CTS-PCL fibers to regenerate nerve tissue. They demonstrated that aligned CTS-PCL fibrous scaffolds directly connected to Schwann cell attachment exhibited better nerve regeneration performance than CTS-PCL film and randomly oriented fibers. This study suggests that CTS-PCL fibers provide chemical and topographical cues for modulating neurogenesis and may serve as a potential scaffold for nerve regeneration[198].

Nerve tissue regeneration typically requires a flexible tubular scaffold (to prevent compression of the regenerating nerve), biocompatible, mechanically stable during nerve regeneration, porous to ensure nutrient supply, and degradable into non-toxic products. In a 2013 study by Liao et al., multi-channel CTS-PCL channels fixed with microspheres were used to control nerve growth factor release. This research demonstrated that CTS and PCL can carry and control the release of nerve growth factors through their channels, preserving the bioactivity of entrapped NGF and administering its release at approximately linear rates for over 6 weeks. The optimized multi-channel conduits, with dimensions of approximately 6 mm in outer diameter and 30 mm in length, exhibited capable compressive resistance in the wet state and tunable in vitro degradation rates. These results indicate that the currently designed multi-channel conduits embedded with microspheres may be potential implants for bridging longer nerve gaps [199].

In 2016, Bolaina and colleagues utilized electrospun PCL and CTS scaffolds for nerve tissue engineering, investigating the structure of scaffolds and their biocompatibility properties at varying amounts of CTS. As demonstrated by Akbari et al. in 2008, this study also confirmed that CTS alongside PCL reduced the contact angle from 130 to 52 degrees and increased hydrophilicity. Additionally, cell attachment results indicated that the highest amount of cell adhesion occurred with 5 wt% CTS, though the amount of cell adhesion with CTS (5wt%)/PCL was better than with 5 wt% CTS alone.

Studies have shown that electrical stimulation plays a significant role in stimulating nerve regeneration and cell proliferation. Various electrically conductive scaffolds have been utilized to promote nerve regeneration at the site of injury[200, 201]. Among the types of inorganic materials used for repairing damaged nerve tissue, gold nanoparticles (AuNPs) are a potential candidate due to their unique optical and electronic characteristics and excellent biocompatibility. To prepare gold nanoparticles, reducing and stabilizing gold salts is necessary. CTS performs this dual role, stabilizing and reducing AuNPs from HAuCl4 through its hydroxyl and amino groups[202]. CTS electrospinning has limitations such as low mechanical strength, limited solubility, and a poly-cationic nature in solution. PCL addresses these limitations, while CTS improves PCL's hydrophilic properties and biological limits.

In 2018, Saderi et al. utilized gold nanoparticle-doped electrospun PCL-CTS nanofibrous scaffolds for nerve tissue engineering. In this research, PCL-CTS mixtures with varying

concentrations of CTS (0.5, 1, and 1.5) were electrospun to produce nanofibrous scaffolds. As the concentration of CTS increased, the diameter of the nanofibers decreased from 180 to 123 and 114 nm, respectively.

Evaluations have shown that incorporating AuNPs significantly enhances scaffolds' conductivity. A cell culture study conducted over 5 days on PCL-CTS scaffolds, both with and without AuNPs, demonstrated the ability of both scaffolds to support the proliferation of Schwann cells. Additionally, the significant amount of Schwann cell adhesion on the PCL-CTS nanofibrous scaffolds indicates their promising potential for regenerating damaged nerves[203].

In a 2021 study, Pooshidani et al. fabricated and characterized porous and conductive nanofibers of PCL/CTS doped with AuNPs. In addition to the presence of CTS, the reducing agents phosphonium chloride (THPC) and formaldehyde were used to improve the stabilization and reduction of AuNPs. To achieve favorable porosity, varying percentages of polyethylene oxide (PEO) were used as sacrificial fibers. The sample with 40% PEO, exhibiting 75-80% porosity after PEO elimination, demonstrated the highest hydrophilicity. This improvement in porosity and hydrophilicity increased cell adhesion, expansion, and proliferation **(Figure 11A)**[204].

Recent studies have shown that immobilized nerve growth factors (NGFs) positively affect budding and neurite outgrowth in various cells. However, the diffusion of NGFs delivered in solution from injury sites often requires injection, making it impractical. Immobilizing NGFs on a scaffold can address this issue[205]. In this regard, Afshar et al. immobilized NGF on CTS-PCL nanofibers using dopamine in 2021 and evaluated their efficacy. The results of this study revealed that aligned PCL-CTS nanofibers could provide the requirements for neural cell growth due to their appropriate physicochemical and topographical features. Better efficiency was achieved by functionalizing the scaffolds with NGFs, a potent agent for nerve regeneration[206].

One of the most intriguing technologies in tissue engineering is 3D printing, which offers numerous possibilities for creating implants with precise shapes, dimensions, mechanical parameters, and permeability. However, scientists face limitations in this technique due to common polymers' high melting temperature and low degradation rate. To address this issue, Nawrotek et al. developed a novel method in 2021 to improve the construction of tubular implants by developing 3D printing methods that employ polymer extrusion and electrophoretic deposition to produce hybrid implants **(Figure 11C)**. Results indicated that the developed

strategy effectively incorporates a PCL skeleton within a CTS-hydroxyapatite hydrogel deposit. The shape flexibility of the extruded PCL construct is a valuable tool for incorporating mechanical or biological signals that promote cell growth, guidance, and proper axon targeting. The results showed that the implants produced did not change significantly over 28 days at 37 degrees Celsius, indicating promising performance in 3D printing **(Figure 11B)**[207].

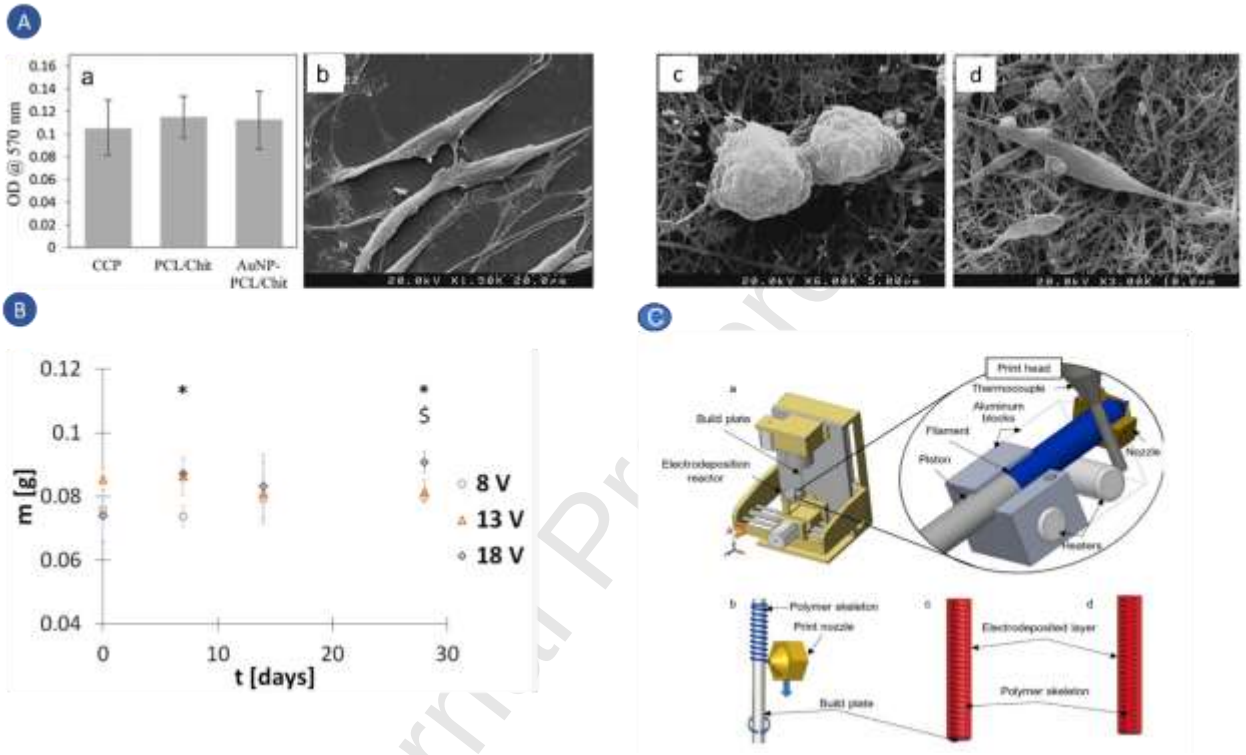

Figure 11: A) An MTT assay was conducted to observe the proliferation of Schwann cells. These cells were cultured on a cell culture plate (CCP), PCL/CTS and PCL/CTS scaffolds decorated with AuNPs (AuNP-PCL/CTS). The observation was made 48 hours post-cell seeding. **B)** FESEM micrographs were used to visualize Schwann cells on a tissue culture plate **(a)** and AuNPs-decorated PCL/CTS scaffolds. These scaffolds were fabricated using THPC and formaldehyde **(b and c)**. The mature Schwann cells exhibited their characteristic spindle-shaped morphology with long processes. This was observed on the tissue culture plate and the AuNPs decorated PCL/CTS scaffolds. Additionally, there was evidence of Schwann cell proliferation on the AuNPs-decorated PCL/CTS scaffolds**(d)**[34]. **B)** Hybrid implants were incubated in PBS with a pH of 7.4 at 37 °C for designated durations. The mass of these implants was then measured. The symbols * and $ denote significant differences between the groups of implants. These implants were obtained through electrodeposition at 8 V and 18 V, and 13 V and 18 V, respectively, with a significance level of $p < 0.05$[207]. **C) (a)** The device is designed to create hybrid implants based on polymer extrusion and electrophoretic deposition techniques. The manufacturing process follows a specific sequence of steps. The processes involved are **(b)** the polymer extrusion process, **(c)** the electrodeposition process, and **(d)** the fabrication of a hybrid implant[207].

3.13. Bladder

The bladder is a hollow, musculomembranous, uneven organ that collects urine from the kidneys, conveyed by the ureters. It functions as a temporary reservoir, filling between urinations and periodically emptying to eliminate accumulated urine through the urethra. Current clinical strategies for bladder reconstruction or substitution are associated with severe problems, necessitating new alternative approaches. Tissue bladder engineering requires a biocompatible material capable of sustaining the mechanical forces necessary for bladder filling, a compliant muscular wall, and a highly specialized urothelium under the control of autonomic and sensory innervations[208].

Baker et al. evaluated the mechanical properties of biodegradable PCL foam scaffolds (85-88% porosity) and stromal cell behavior on them, demonstrating that these scaffolds may be highly suitable for soft tissue and bladder tissue engineering[209].

PCL was blended with CTS (2:8) to prepare a scaffold for bladder reconstruction using a vacuum freezing and drying manufacturing method. The resulting scaffolds (porosity 88.94 ± 2.14%) were seeded with adipose-derived stem cells (ASCs) for bladder augmentation **(Figure 12)** [210]. 8 weeks after implantation using a rat bladder augmentation model, the experimental group exhibited more densely packed smooth muscles, a larger bladder capacity, and more intensive blood vessels. Immunofluorescence staining also demonstrated that some smooth muscle cells had transdifferentiated from the ASCs. These encouraging results indicate that ASCs promote bladder smooth muscle regeneration through transdifferentiation and participation in neovascularization.

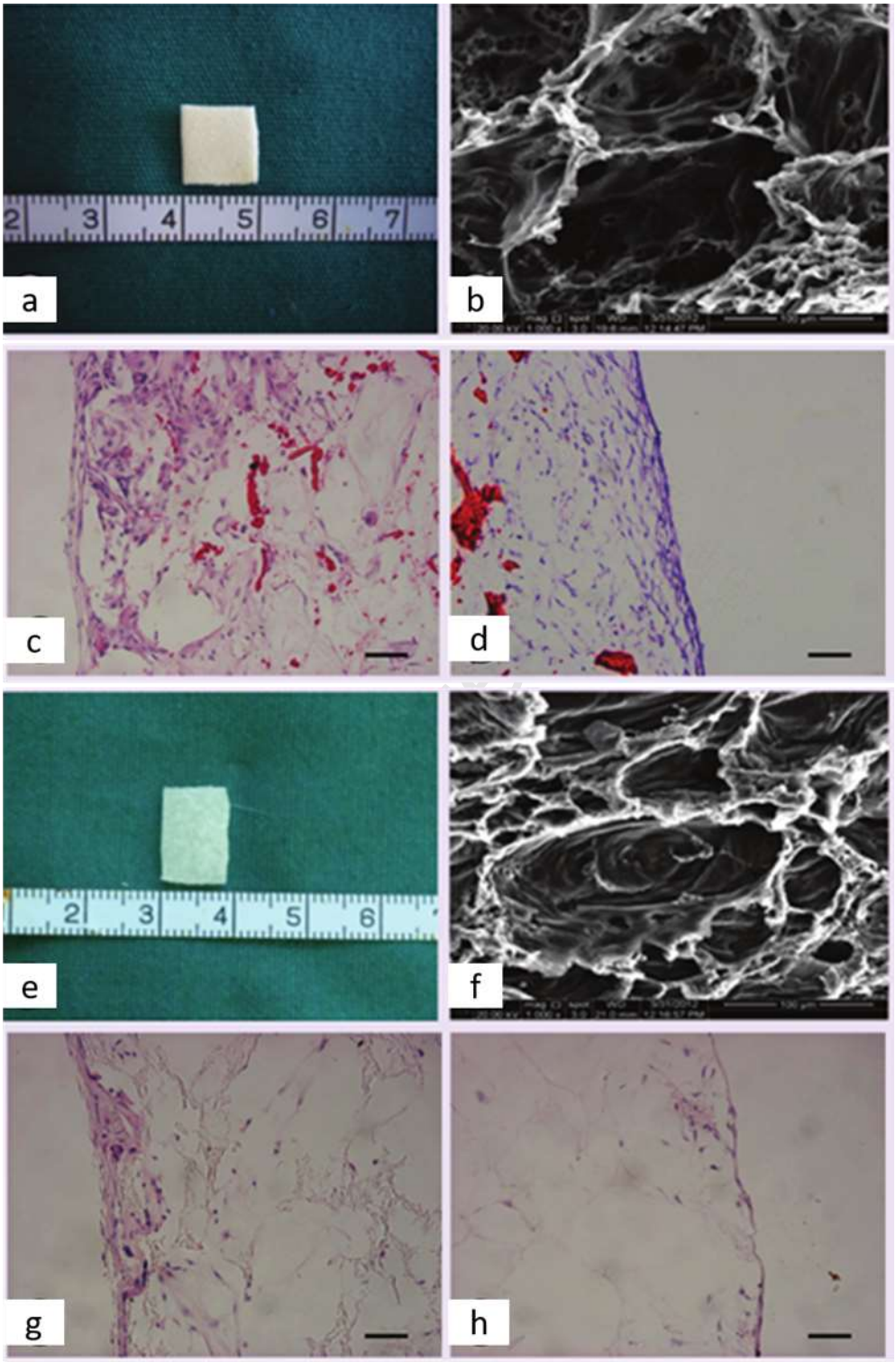

Figure 12: Morphology and biocompatibility of the PCL/CTS and PCL scaffold. The PCL/CTS **(a)** and the PCL **(e)** scaffold appeared as a white membrane in gross view. Scanning electron microscopy analyses demonstrated the porous structure of the PCL/CTS (b) and PCL **(f)** scaffold. Hematoxylin and eosin staining suggested better biocompatibility of the PCL/CTS (c-d) than the PCL **(g-h)** scaffold both in vivo **(C & G)** and in vitro **(D&H)**. Scale bar = 100 µm[211].

PCL and CTS were combined to prepare cationic nanoparticles for encapsulating the intravesical chemotherapeutic agent Mitomycin C (MMC), providing longer residence time, higher local drug concentration, and prevention of drug loss during bladder discharge[212]. Compared to uncoated PCL nanoparticles and poly-L-lysine coated PCL nanoparticles, PCL nanoparticles coated with the bioadhesive polymer CTS exhibited favorable drug loading and release profiles, as well as good cellular interaction and anticancer efficacy[213]. CTS has emerged as a coating material for bioadhesive intravesical drug delivery systems and a preferred material for designing nanoparticles and scaffolds for bladder applications.

3.14. Digestive system

The digestive system comprises a series of organs and structures responsible for ingesting, processing, and absorbing food and eliminating undigested food residues. It includes the mouth, epiglottis, pharynx, esophagus, stomach, small intestine, and large intestine.

Tissue engineering techniques are increasingly surpassing traditional organ transplant treatments, with numerous strategies currently being investigated to regenerate various parts of the digestive tract. A TE approach for the gastrointestinal tract must consider four fundamental aspects: i) designing an appropriate scaffold, ii) cellularizing the scaffold with the correct cells, iii) ensuring construct maturation in bioreactors, and iv) implanting the construct in vivo and supporting physiological functions[214]. Scaffolding biomaterials used for digestive system engineering typically include collagen, CTS, poly-l-lactic acid (PLA), polyglycolic acid (PGA), composites of PLA and PGA, and PCL. Due to its intrinsic mucoadhesive property, CTS is helpful for therapeutic and regenerative applications in the digestive system[215]. Additionally, it has effects on intestinal motility, scavenges fat and cholesterol in the gastrointestinal system, and stimulates the immune system[216].

PCL is an aliphatic polyester with a highly crystalline structure, providing good mechanical resistance. However, it has low surface energy, poor hydrophobicity, and a slow degradation rate[217]. Blending PCL and CTS allows for the exploitation of the properties of both biopolymers, which cannot be achieved individually, to obtain an optimal scaffold for tissue engineering and digestive system applications[218].

3.14.1. Dental

Research on PCL-CTS composite scaffolds is still in its early stages. It has been reported that CTS enhances wettability and permeability, accelerates PCL hydrolytic degradation, and promotes PCL cell recognition sites[219].

PCL-based synthetic polymers improve the mechanical properties of natural polymers such as CTS and have shown promising results in calcified tissue engineering[220].

Both polymers have been used to fabricate porous scaffolds that provide a 3D microenvironment for the adhesion, proliferation, and differentiation of human dental pulp stem cells (hDPSCs). SEM images confirm the suitability of the fabricated PCL/CTS scaffold for the adhesion and proliferation of hDPSCs[221]. Both polymers have been utilized to produce porous scaffolds that provide a 3D microenvironment for the adhesion, proliferation, and differentiation of hDPSCs. SEM images confirm the suitability of the fabricated PCL/CTS scaffold for the adhesion and proliferation of hDPSCs[222].

CTS possesses antimicrobial and immunomodulatory properties, is biocompatible and biodegradable, and has been used as a drug delivery strategy. For example, it has been observed that 5% CTS nanoparticles are capable of inhibiting the oral bacteria Staphylococcus in vitro[222].

Therefore, several approaches have proposed its use in combination with other polymers. PCL is also used with painkillers to reduce toothache. Scaffolds composed of CTS, pectin, and CTS-pectin were prepared and blended with nanostructured lipid carriers (NLC) and loaded with a eutectic mixture of 5% lidocaine-prilocaine (LDC-PLC)[223].

PCL has been used with alginate for drug release during dental treatments to prevent bacterial accumulation at the implantation site. PCL has also been utilized in drug delivery to produce membranes incorporating nano-hydroxyapatite and amoxicillin, reducing bacterial contamination of periodontal defects. PCL scaffolds mineralized with apatite enhance cell proliferation in dental pulp[224].

The presence of 10% β-TCP nanoparticles in the fibers increased hydrophilicity, bioactivity, biodegradability, mechanical properties, and higher cell proliferation compared to PCL/PGS nanofibrous membranes. The incorporation of CTS into PCL/PGS nanofibers as a GTR membrane was found to increase hydrophilicity and degradation rate[225].

Based on the results of a recent study, it can be concluded that bFGF-loaded PCL/CTS scaffolds can promote angiogenesis of hDPSCs, potentially providing pulp vitality as an initial requirement for pulp regeneration [225].

The PCL/HA/CTS scaffold exhibited the lowest water contact angle and the highest level of hydrophilicity among the developed scaffolds. Thus, it can be proposed that the fabricated PCL/FHA/CTS scaffold meets the primary requirements for suitability as a scaffold for dental tissue engineering applications[226]. Mineral trioxide aggregate (MTA) holds the potential for regenerative applications, particularly as a material for root repair. This makes it a promising candidate for future developments in regenerative dentistry. Creating scaffolds based on MTA could offer a viable alternative for procedures in regenerative endodontics. These MTA-based scaffolds have been successfully produced and have proven to be an appropriate structure for the attachment and growth of hDPSCs. Moreover, when hDPSCs were seeded on the PCL/CTS/MTA scaffold, there was an observed increase in their angiogenic potential[227].

Toxicity testing against dental pulp stem cells revealed that the developed materials are biocompatible, with cell activity above 70% compared to the negative control. As a result, CTS-xanthan-PCL scaffolds have great potential for use as periosteum substitutes, as they can be easily obtained and applied, replicating the tissue's natural characteristics and meeting the requirements for various applications [228]. Various PCL/CTS/gelatin membrane samples were created by adding different amounts of β-TCP to investigate their biocompatibility and osteogenic properties for potential GTR/GBR applications. The PCL/CTS/gelatin/β-TCP substrate with 3% β-TCP was considered a promising material candidate for generating bone in GBR applications **(Figure 13A)**[229].

3.14.2. Mouth

The mouth, or oral cavity, is the initial part of the gastrointestinal tract and serves as the opening through which humans ingest food and produce vocal sounds. A decline in oral health can result in facial and functional alterations, severe microbial infections, and malnutrition[230]. Local pharmacological treatments have been studied to reduce or eliminate oral cavity pathologies. Mucoadhesion has emerged as a potential strategy for improving in situ drug delivery by prolonging the residence time of dosage forms at mucosal membranes[231].

Mazzarino et al. studied the effect of CTS-decorated PCL nanoparticles loaded with curcumin to improve buccal delivery for local disease treatments, such as oral lesions and carcinomas. The influence of three different CTS molar masses (low, medium, and high) was monitored regarding interaction with the mucin layer using Quartz Crystal Microbalance with Dissipation Monitoring (QCM-D). CTS-coated PCL nanoparticles were prepared using the nanoprecipitation method and characterized by Dynamic Light Scattering (DLS) for their size and Z-potential. Uncoated PCL nanoparticles (105nm, neutrally charged) exhibited no affinity for the bovine submaxillary gland mucin layer (negatively charged). In contrast, CTS-coated nanoparticles (120nm, positively charged) showed higher affinity with the mucin layer, but no significant behavior was observed between the three different CTS molar masses used for nanoparticle decoration. This led to the conclusion that CTS molar mass does not influence the adsorption of CTS-coated nanoparticles on the mucin layer **(Figure 13B)**. Results confirmed that the mucoadhesive characteristics of the proposed systems are solely attributed to their decoration with CTS and suggested that CTS-coated PCL nanoparticles are promising carriers for hydrophobic drug delivery in the buccal mucosa[232]. Mazzarino's work was expanded upon by investigating the effect of mucoadhesive films in prolonging the residence time of dosage forms in the oral cavity and increasing drug absorption through the buccal mucosa[233]. Mucoadhesive films were prepared using the casting method after incorporating curcumin-loaded CTS-coated PCL nanoparticles into plasticized CTS solutions. Incorporating nanoparticles into mucoadhesive films allowed for the controlled delivery of the loaded drug directly to the application site for prolonged periods (> 24h). CTS at medium and high molar mass used for film preparation exhibited superior results in terms of homogeneity, flexibility, and thickness for oral application. Furthermore, the use of CTS for both film and nanoparticle coating preparation may improve drug bioavailability due to its ability to increase molecule penetration across the mucosal surface.

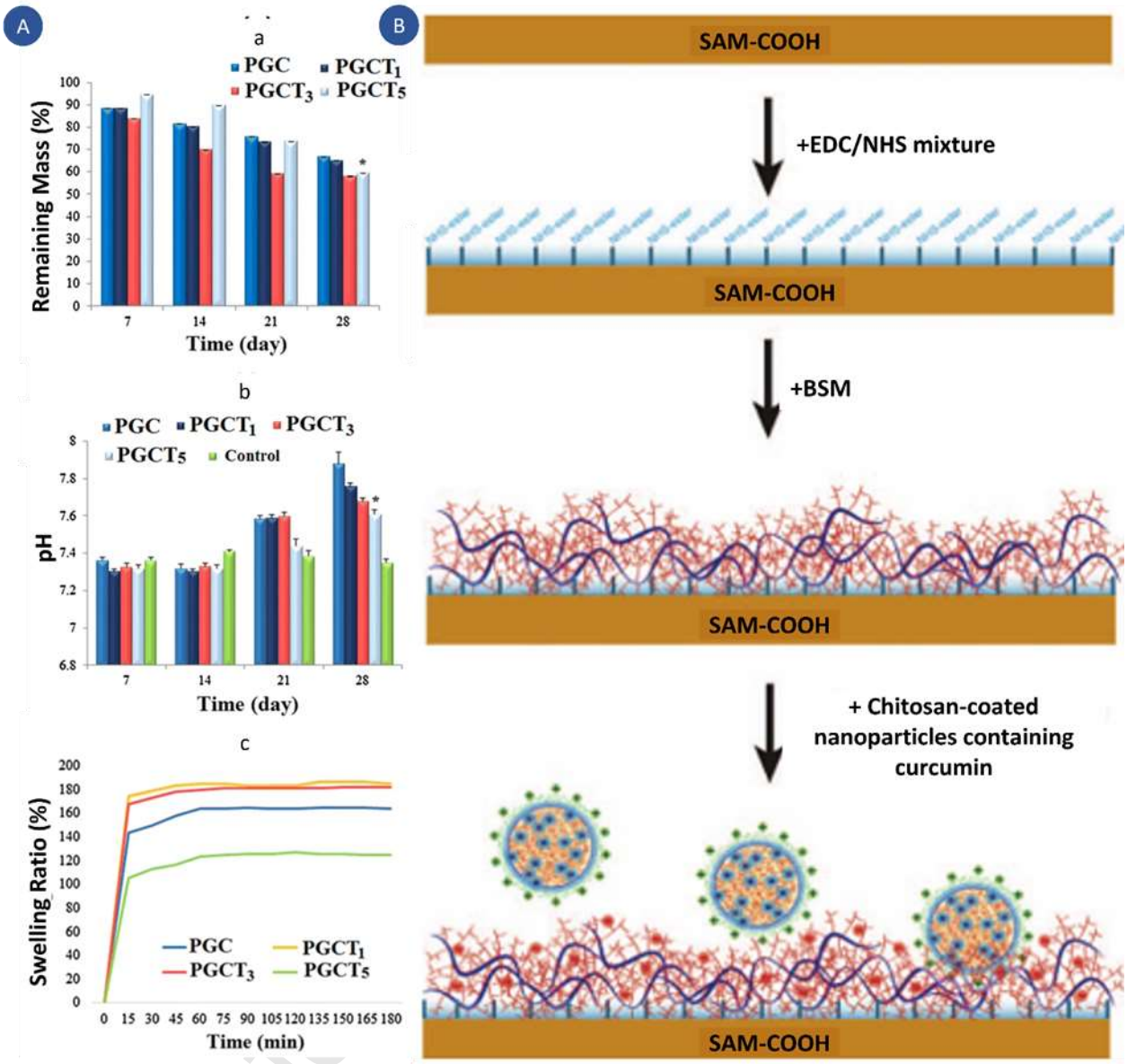

Figure 13: A) The weight loss **(a)** and micro-environmental pH variation **(b)** of samples during 4 weeks incubation in PBS, *P < 0.05, compared to other samples. Dynamic swelling behavior of the samples after immersion in PBS at 37 °C **(c)**[234]. **B)** Schematic representation of mucin immobilization on the gold surface followed by adsorption of CTS-coated nanoparticles[37].

In cases where more substantial regenerative intervention is required for oral cavity pathologies, tissue engineering techniques are evolving to develop scaffolds capable of adapting to the varying needs of patients[235].

Fused Deposition Molding (FDM) 3D printing was utilized to create a PCL-CTS-based implant for personalized drug delivery and facial plastic surgery[236]. The support material was PCL, while Ibuprofen and CTS functioned as plasticizers. These plasticizers weakened the PCL

matrix's intermolecular forces and reduced interchain entanglements, decreasing tensile strength. The implant's morphology revealed suitable interfacial adhesion and compatibility between the drug and the PCL matrix, ensuring prolonged release (120h) through a diffusion-erosion mechanism. CTS was well integrated with the matrix and uniformly distributed, increasing the implant's surface roughness. The results suggest that PCL-CTS filaments can be manufactured as an implant for controllable and efficient sustained drug release in personalized medicine administration.

3.14.3. Esophagus

The esophagus, a hollow fibromuscular tube, transports food and liquid from the pharynx to the stomach. Despite various tissue engineering strategies being employed to replace esophageal defects with natural or artificial substitutes engineered with cells and/or active molecules, a gold standard for esophageal reconstruction remains elusive **(Figure 14A)**[237].

A polymeric patch was created using a temperature-induced precipitation method, combining synthetic polylactide-co-polycaprolactone (PLA:PCL 70:30) and CTS biopolymers to produce multilayered patches with properties tailored to esophageal tissue characteristics[238]. Results demonstrated the feasibility of obtaining multilayered patches by combining and modulating different polymers. The manufacturing process ensured scaffold porosity of approximately 80% or higher. Biological characterization revealed higher cell viability values for patches prepared with PLA:PCL (200mg)/ CTS (20mg) and mechanical properties capable of withstanding physiological esophageal stress. A preliminary ex vivo suture test on a pig's esophagus confirmed the patch's resistance and suturability.

The same biopolymers, PLA:PCL 70:30 and CTS, were utilized to produce polymeric electrospun nanofibers via the electrospinning technique for tissue engineering and esophageal tissue applications [239]. Results demonstrated the production of homogeneous and defect-free nanofibers with a diameter of 800nm, ensuring suitable nutrient permeation (Mw of 180Da and 5900Da) through the fiber network. CTS (27 wt%) enhanced membrane hydrophilicity, cell attachment, and proliferation without compromising the entangled nanofiber structure and stability.

The advent of 3D printing and 3D bioprinting techniques has influenced the development of scaffolds for esophageal regeneration[240]. A study investigated the efficacy of a 3D-printed PCL scaffold loaded with an antibiotic drug in pharyngoesophageal reconstruction and sustained drug release[241]. The scaffold demonstrated the ability to prevent saliva leakage and exert an antimicrobial effect, with muscle regeneration observed around the graft sites in the group containing 1% and 3% tetracycline. Reepithelialization, neovascularization, and elastin production were also identified around the implanted sites. Implementing CTS, which possesses intrinsic antimicrobial activity, could further enhance the scaffold's antimicrobial and regenerative capabilities.

3.14.4. Stomach

The stomach, a muscular organ that receives food from the esophagus, performs several key functions, including serving as a reservoir, secreting acid and enzymes, and promoting gastrointestinal motility[242]. Diseases affecting the stomach, such as gastritis, gastroparesis, Crohn's disease, and various cancers, typically present with a range of symptoms, including heartburn or epigastric pain[243]. Bioengineered stomachs have not yet proven safe and effective due to complications in resuming the continuity of the GI tract, the invasiveness of surgical procedures, and post-operative maintenance. However, efforts have been made to regenerate the stomach or portions of it using tissue engineering strategies[214].

PCL/CTS, due to their biocompatibility, were chosen as base materials for the production of stents to prevent anastomotic leakage following gastrointestinal surgery[244]. Lends of PCL/CTS in ratios of 50:50, 60:40, 70:30, and 80:20 wt/wt% were molded into stent shapes and characterized for their mechanical properties, demonstrating the producibility of PCL/CTS stents with a wide range of strain at failure and mechanical strengths. Tensile results revealed that increasing the amount of CTS in the blend increased strain and mechanical strength. Furthermore, PCL/CTS stents are biodegradable and do not require surgical removal, reducing surgical complications and patient mortality.

Another function of the stomach is the absorption of orally administered drugs, which can be impaired in cases of common diseases such as abdominal irritation, diarrhea, nausea, tachycardia, palpitations, and hypertension[245]. It is possible to develop controlled drug delivery systems (DDS) within specific gastrointestinal (GI) tract sections to ensure suitable

pharmacological treatment while avoiding invasive regenerative interventions[246]. Hussain et al. developed gastro-retentive swellable mucoadhesive matrix tablets using a modified solvent-based wet granulation method by mixing milnacipran (MCN), low molecular weight CTS (CTS-LM), medium molecular weight CTS (CTS-MM), and PCL [247, 248]. A design of experiment (DoE) approach was employed to formulate a gastro-retentive mucoadhesive sustained-release matrix for milnacipran (MCN), a water-soluble serotonin-norepinephrine reuptake inhibitor used in the clinical treatment of fibromyalgia[40]. The optimized formulation, developed by combining CTS and PCL, exhibited improved in vitro mucoadhesion, appropriate water uptake, controlled swelling properties, and porosity following a non-Fickian diffusion type of drug release mechanism[249]. Their work confirmed the advantages of blending CTS and PCL to obtain a mucoadhesive gastro-retentive matrix system that could also be applied to other GI disorders using the oral administration route.

3.14.5. Intestine

The human intestine, a tube approximately ten meters long, is located within the abdominal cavity and enveloped by the peritoneum membrane, forming loops or intestinal convolutions. The intestine is organized into crypts and villi containing stem cells and differentiated cells, respectively. Furthermore, the intestine is the most highly regenerative organ in the human body, with the intestinal epithelium undergoing constant renewal every five to seven days[250]. However, mechanical stress, infections, chronic inflammation, or cytotoxic therapies can damage the intestinal stem cell niche, resulting in a loss of self-renewal function[251].

Polymeric micelles, formed through the self-assembly of amphiphilic macromolecules, are commonly used in oral administration to improve drug permeability through the gastrointestinal (GI) mucosa and reduce the cytotoxic effects of certain drugs, such as chemotherapy[252]. Self-assembled amphiphilic micelles based on CTS (2% w/v) and PCL (1g) were produced as carriers for paclitaxel (PTX) to enhance its intestinal pharmacokinetic profile[253]. Micelles produced using the solvent evaporation method exhibited a mean particle size of 408nm, a narrow size distribution (polydispersity index of 0.335), and a positive surface charge of approximately 30mV, resulting in a high PTX association efficiency of 82%. In-vitro cytotoxicity testing of unloaded and PTX-loaded micelles against Caco-2 and HT29-MTX intestinal epithelial cells revealed no cell toxicity for any formulation, unlike the free drug, which exhibited evident

toxicity patterns. Furthermore, micelles improved the intestinal permeability of PTX in two intestine cell-based models (Caco-2 monolayer and Caco-2/HT29-MTX co-culture model), with more pronounced effects in the presence of mucus, highlighting the mucoadhesive properties of PCL/CTS micelles as potential drug carriers for the intestinal delivery of hydrophobic drugs, particularly anticancer agents.

In a study conducted by Gu et al., a graft copolymer (CTS-graft-poly-ε-caprolactone) was self-assembled into micelles as a delivery system for the drug 5-fluorouracil (5-Fu)[254]. The resulting micelles exhibited good biocompatibility, with 5-Fu loaded micelles displaying lower cytotoxicity due to the slow release of encapsulated 5-Fu from the micelles (50h) compared to the free drug (10h). Furthermore, free 5-Fu and 5-Fu-loaded micelles successfully efficiently kill cancer cells (A549 cells).

Hadjianfar et al. utilized 5-Fu blended in PCL/CTS electrospun nanofibers to create an anticancer drug delivery system for colorectal cancer[255]. Their study demonstrated that the proportion of PCL-CTS (0:1 to 5:1) significantly affected release behavior, mechanical properties, and nanofiber morphology. Smaller fiber dimensions were obtained using less CTS. Increasing the proportion of CTS resulted in an increased nanofiber degradation rate, drug encapsulation efficiency, and drug release time. 5-Fu was released from the nanofibers through a Fickian diffusion mechanism according to the Korsmeyer-Peppas model. This anticancer drug delivery system aims to reduce side effects on healthy organs and achieve appropriate drug concentrations around cancer cells.

In cases where segments of the intestinal tract are damaged or diseased, surgical intervention and extensive resection may be required. Surgical alternatives using cellularized scaffolds are being developed to avoid using autologous tissue portions. In various studies, CTS and PCL were utilized as biomaterials to support smooth muscle constructs and small intestinal epithelial cells in intestinal tissue engineering applications **(Figure 14B)**[256, 257]. Forming aligned smooth muscle constructs is beneficial for restoring intestinal motility and propelling intestinal content, while suitable re-epithelialization is essential for ensuring integration and uniformity with surrounding tissues.

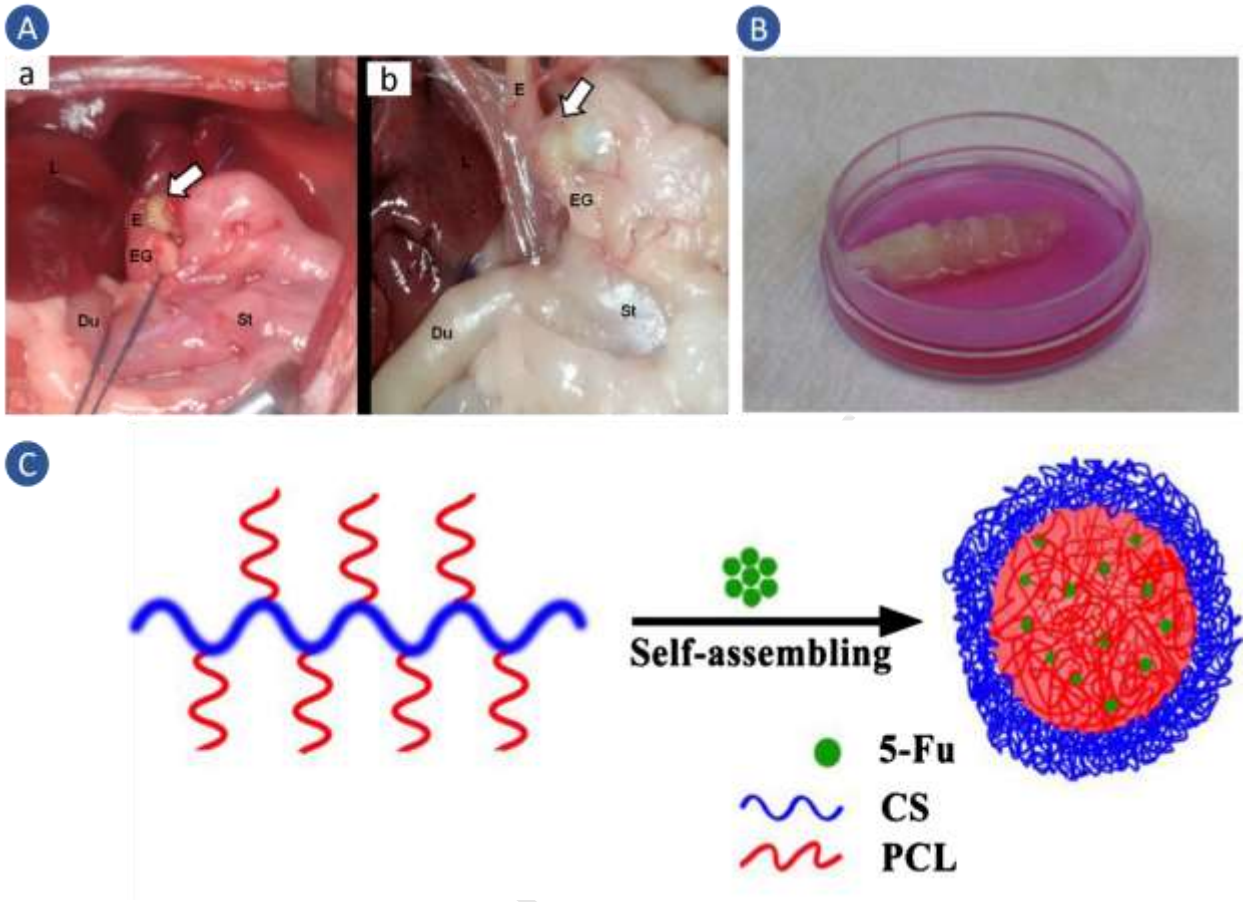

Figure 14: A) (a) The surgical site of transplantation. **(b)** The transplanted site is 30 days after transplantation. Arrows: transplanted site, Du: duodenum, E: esophagus, EG: esophagogastric junction, L: liver, St: stomach[39]. **B)** Four bioengineered constructs were mounted around the composite CTS tubular scaffold and maintained in culture for 2 weeks. Tissue constructs were placed 1 mm apart[256]. **C)** Preparation of micelles composed of chitosan-graft-poly(ε-caprolactone) amphiphilic copolymers derived from polysaccharides[258].

Chunhua Gu et al. [258] conducted a study where they synthesized CTS-PCLs with varying grafting levels of ε-CL repeating units. This was achieved using ring-opening graft polymerization of ε-caprolactone onto the hydroxyl groups of C-S. Methanesulfonic acid was used as the solvent and catalyst in this process. Subsequently, polymeric micelles were created and utilized to encapsulate 5-Fu using the dialysis ap proach. The results demonstrated that the release of 5-Fu was manageable and significantly slower compared to the discharge of free 5-Fu. The evaluation of cytotoxicity and the investigation of cellular death indicated that CS-g-PCL micelles have excellent biocompatibility. In addition, micelles loaded with 5-Fu were able to slow down the release of the medication and demonstrate similar lethal effects on A549 cells **(Figure 14C)**.

Huang et al. developed a novel antiadhesion membrane composed of PCL, gelatin, and CTS (PGC) using the electrospinning technique [259]. The PGC electrospun membrane may serve as a potential peritoneal antiadhesion barrier for clinical use to prevent common adverse effects such as chronic pelvic pain, intestinal obstruction, and infertility. Membranes were prepared using varying amounts of CTS (0%, 0.5%, 1%, and 2% wt%), with results indicating that PGCS with higher CTS content (PGC2) exhibited better antiadhesion effects, as evaluated by an adhesion score at day 14 post-surgery following implantation between the cecum and peritoneal wall defects in a rat model. Thus, electrospun PGC2 effectively reduces tissue adhesion formation and holds great potential for clinical peritoneal antiadhesion applications.

4. Conclusion

To recapitulate, employing PCL and CTS-based scaffolds within tissue engineering has yielded promising outcomes for regenerating diverse tissue types. These biocompatible and biodegradable polymers have enabled scaffold creation featuring favorable attributes like improved hydrophilicity, mechanical robustness, and biodegradability. Furthermore, these materials have showcased the ability to incite cell growth and differentiation, making them suitable for regenerative medicine endeavors.

When PCL and CTS are combined, they synergistically enhance the properties of each polymer, resulting in superior outcomes for tissue engineering applications. Continued investigation is warranted to refine the implementation of PCL-CTS-based scaffolds across varied tissue engineering scenarios, harnessing their potential to elevate patient outcomes.

Integrating biocompatible and biodegradable polymers like PCL, CTS, and gelatin alongside materials like β-TCP has yielded encouraging advancements in tissue engineering and drug delivery domains. These materials have been used to construct scaffolds, membranes, and drug delivery systems with sought-after qualities, including heightened hydrophilicity, mechanical resilience, and biodegradability. Moreover, these materials have exhibited compatibility with living systems and the capacity to instigate cell growth and specialization, positioning them favorably for utilization in regenerative medicine. Further inquiry remains essential to fine-tune the application of these materials across diverse contexts, unlocking their full potential to enhance patient outcomes.

This research elucidates the global scientific consensus on applying the composite made from PCL and CTS in different organs (Table 1). This composite is a leading material in the field of tissue engineering for a variety of body tissues. Considering the organ of interest, it offers a valuable perspective on the properties and optimal ratios for creating this composite. This study significantly enhances the scientific community's comprehension and utilization of PCL-CTS in tissue engineering. It sets the stage for future research to fine-tune the composite's attributes and manufacturing techniques for specific organ applications. This progress will undoubtedly catalyze breakthroughs in tissue engineering and regenerative medicine. However, the technical parameters mentioned, such as perplexity score, burstiness score, complexity score, temperature, frequency penalty, presence penalty, scientific score, predictability score, probability score, and pattern score, are not applicable in this context as they pertain to machine learning models and not to the process of scientific writing or paraphrasing.

Acknowledgment

No particular grant from any institution or organization was obtained for this work. We are grateful for TISSUEHUB Co.'s research assistance.

Conflict of Interest

The authors state that there is no conflict of interest.

Author contribution

Javad Esmaeili: Conceptualization, Methodology, Validation, Investigation, Data Curation, Writing - Review & Editing, Supervision, Project administration, Revision. **Saeedeh Zare Jalise:** Validation, Investigation, Writing - Original Draft, Writing - Review & Editing, Revision. **Silvia Pisani:** Investigation, Writing - Original Draft. **Gaël Y. Rochefort:** Investigation, Writing - Original Draft. **Farbod Ghobadinezhad:** Investigation, Writing - Original Draft. **Zeynab Mirzaei:** Investigation, Writing - Original Draft. **Riaz Ur Rehman Mohammed:** Investigation, Writing - Original Draft. **Mehdi Fathi:** Edition, Revision**. Amir Tebyani:** Investigation, Writing - Original Draft. **Zohreh Mousavi Nejad:** Investigation, Writing - Original Draft.

References

1. D. Semnani, E. Naghashzargar, M. Hadjianfar, F. Dehghan Manshadi, S. Mohammadi, S. Karbasi and F. Effaty, *International Journal of Polymeric Materials and Polymeric Biomaterials*, 2017, **66**, 149-157.
2. H. Zhang, X. Luo, X. Lin, X. Lu, Y. Zhou and Y. Tang, *Materials & Design*, 2016, **90**, 396-402.
3. H.-H. Kao, C.-Y. Kuo, D. Tagadur Govindaraju, K.-S. Chen and J.-P. Chen, *International Journal of Molecular Sciences*, 2022, **23**, 9517.
4. S. Abuelreich, M. Manikandan, A. Aldahmash, M. Alfayez, M. F. Al Rez, H. Fouad, M. Hashem, S. Ansari, F. F. Al-Jassir and A. Mahmood, *Journal of Nanoscience and Nanotechnology*, 2017, **17**, 1771-1778.
5. S. Gomes, G. Rodrigues, G. Martins, C. Henriques and J. C. Silva, *International journal of biological macromolecules*, 2017, **102**, 1174-1185.
6. C. O'Leary, L. Soriano, A. Fagan-Murphy, I. Ivankovic, B. Cavanagh, F. J. O'Brien and S.-A. Cryan, *Frontiers in Bioengineering and Biotechnology*, 2020, **8**, 190.
7. D. L. Roman, M. Roman, C. Som, M. Schmutz, E. Hernandez, P. Wick, T. Casalini, G. Perale, V. Ostafe and A. Isvoran, *Frontiers in bioengineering and biotechnology*, 2019, **7**, 214.
8. C. L. Salgado, E. Sanchez, J. Mano and A. Moraes, *Journal of Materials Science*, 2012, **47**, 659-667.
9. C. D. Rai, Prince of Songkla University, 2016.
10. A. R. Sarasam, A. I. Samli, L. Hess, M. A. Ihnat and S. V. Madihally, *Macromolecular bioscience*, 2007, **7**, 1160-1167.
11. Y.-C. E. Li, J.-H. Wang, Y.-H. Wang, H.-J. Shao, L.-C. Young and T.-H. Young, *ACS Biomaterials Science & Engineering*, 2020, **6**, 4225-4235.
12. Y. Zhang, Y. Wu, M. Yang, G. Zhang and H. Ju, *Materials*, 2021, **14**, 5538.
13. I. Sivanesan, N. Hasan, M. Muthu, G. Blessing, J. Gopal, S. Chun, J. Shin and J.-W. Oh, *Polymers*, 2022, **14**, 1587.
14. M. Ahmad, K. Manzoor, S. Ahmad, N. Akram and S. Ikram, in *Applications of nanocomposite materials in orthopedics*, Elsevier, 2019, pp. 253-262.
15. N. Z. Zarith and N. Sultana, *Applied Mechanics and Materials*, 2015, **695**, 203-206.
16. M. L. Bravi Costantino, M. S. Belluzo, T. G. Oberti, A. M. Cortizo and M. S. Cortizo, *Journal of Biomedical Materials Research Part A*, 2022, **110**, 383-393.
17. S. Yang, L. Lan, M. Gong, K. Yang and X. Li, *Journal of Biomaterials Applications*, 2022, **37**, 577-587.
18. M.-A. Rojas-Yañez, C.-A. Rodríguez-González, S.-A. Martel-Estrada, L.-E. Valencia-Gómez, C.-L. Vargas-Requena, J.-F. Hernández-Paz, M.-C. Chavarría-Gaytán and I. Olivas-Armendáriz, *AIMS Materials Science*, 2022, **9**.
19. A. D. Dalgic, D. Atila, A. Karatas, A. Tezcaner and D. Keskin, *Materials Science and Engineering: C*, 2019, **100**, 735-746.
20. J. Prakash, D. Prema, K. Venkataprasanna, K. Balagangadharan, N. Selvamurugan and G. D. Venkatasubbu, *International journal of biological macromolecules*, 2020, **154**, 62-71.
21. M. I. Hassan, T. Sun and N. Sultana, *Journal of Nanomaterials*, 2014, **2014**, 65-65.
22. S. Gautam, A. K. Dinda and N. C. Mishra, *Materials Science and Engineering: C*, 2013, **33**, 1228-1235.
23. W. L. Miller and J. C. Burnett Jr, *Rheumatic Diseases Clinics of North America*, 1990, **16**, 251-260.

24. N. Desbuards, G. Y. Rochefort, D. Schlecht, M.-C. Machet, J.-M. Halimi, V. Eder, J.-M. Hyvelin and D. Antier, *Thrombosis and haemostasis*, 2007, **98**, 614-620.
25. J. Lee, J. J. Yoo, A. Atala and S. J. Lee, *Biomaterials*, 2012, **33**, 6709-6720.
26. B. Chan and K. Leong, *European spine journal*, 2008, **17**, 467-479.
27. D. B. Gurevich, P. D. Nguyen, A. L. Siegel, O. V. Ehrlich, C. Sonntag, J. M. Phan, S. Berger, D. Ratnayake, L. Hersey and J. Berger, *Science*, 2016, **353**, aad9969.
28. M. A. Osman, N. Virgilio, M. Rouabhia, L. E. Lorenzo and F. Mighri, *Journal of Applied Polymer Science*, 2023, e54240.
29. T.-J. Wang, I.-J. Wang, F.-R. Hu and T.-H. Young, *Cornea*, 2016, **35**, S25-S30.
30. T.-J. Wang, I.-J. Wang, S. Chen, Y.-H. Chen and T.-H. Young, *Colloids and Surfaces B: Biointerfaces*, 2012, **90**, 236-243.
31. H. Huang, S. Oizumi, N. Kojima, T. Niino and Y. Sakai, *Biomaterials*, 2007, **28**, 3815-3823.
32. H. Bokura and S. Kobayashi, *European journal of clinical nutrition*, 2003, **57**, 721-725.
33. J. Huling, S.-i. Min, D. S. Kim, I. K. Ko, A. Atala and J. J. Yoo, *Acta biomaterialia*, 2019, **95**, 328-336.
34. Y. Pooshidani, N. Zoghi, M. Rajabi, M. Haghbin Nazarpak and Z. Hassannejad, *Journal of Materials Science: Materials in Medicine*, 2021, **32**, 1-12.
35. M. C. Bonferoni, C. Caramella, L. Catenacci, B. Conti, R. Dorati, F. Ferrari, I. Genta, T. Modena, S. Perteghella and S. Rossi, *Pharmaceutics*, 2021, **13**, 1341.
36. T. Ouchi, G. Orsini, A. George and M. Kajiya, *Journal*, 2022, **10**, 840771.
37. L. Mazzarino, L. Coche-Guérente, P. L. E. Lemos-Senna and R. Borsali, *Journal of biomedical nanotechnology*, 2014, **10**, 787-794.
38. L. Mazzarino, R. Borsali and E. Lemos-Senna, *Journal of pharmaceutical sciences*, 2014, **103**, 3764-3771.
39. Y. Takeoka, K. Matsumoto, D. Taniguchi, T. Tsuchiya, R. Machino, M. Moriyama, S. Oyama, T. Tetsuo, Y. Taura and K. Takagi, *PLoS One*, 2019, **14**, e0211339.
40. J. A. Kyle, B. D. Dugan and K. K. Testerman, *Annals of Pharmacotherapy*, 2010, **44**, 1422-1429.
41. F. Hao and X. Maimaitiyiming, *ChemistrySelect*, 2022, **7**, e202200201.
42. J. I. Lim, *3D Printing and Additive Manufacturing*, 2023, **10**, 1072-1079.
43. M. Yoshida, P. R. Turner, C. J. McAdam, M. A. Ali and J. D. Cabral, *Biopolymers*, 2022, **113**, e23482.
44. I. Zarandona, C. Bengoechea, E. Álvarez-Castillo, K. de la Caba, A. Guerrero and P. Guerrero, *Gels*, 2021, **7**, 175.
45. D. Poddar, M. Majood, A. Singh, S. Mohanty and P. Jain, *Progress in Biomaterials*, 2021, **10**, 281-297.
46. F. Liu, W. Li, H. Liu, T. Yuan, Y. Yang, W. Zhou, Y. Hu and Z. Yang, *Macromolecular Bioscience*, 2021, **21**, 2000398.
47. E. Filová, B. Jakubcová, I. Danilová, E. K. Kostakova, T. Jarosikova, O. Chernyavskiy, J. Hejda, M. Handl, J. Beznoska and A. Necas, *Physiological research*, 2016, **65**, 121.
48. N. Omidvar, F. Ganji and M. B. Eslaminejad, *Journal of biomedical materials research Part A*, 2016, **104**, 1657-1667.
49. A. Seddighian, F. Ganji, M. Baghaban-Eslaminejad and F. Bagheri, *Progress in Biomaterials*, 2021, **10**, 65-76.
50. M. J. Rashid, L. Ali Reza and N. Sultana, *Applied Mechanics and Materials*, 2015, **695**, 199-202.
51. X. Jing, H.-Y. Mi, T. Cordie, M. Salick, X.-F. Peng and L.-S. Turng, *Industrial & Engineering Chemistry Research*, 2014, **53**, 17909-17918.
52. K. Kosowska, J. Krzysztoforski and M. Henczka, *Materials*, 2022, **15**, 3858.

53. A. Dhuri, A. Sriram, M. Aalhate, S. Mahajan, K. K. Parida, H. Singh, U. Gupta, I. Maji, S. K. Guru and P. K. Singh, *Pharmaceutical Development and Technology*, 2023, **28**, 460-478.
54. O. R. Guadarrama-Escobar, P. Serrano-Castañeda, E. Anguiano-Almazán, A. Vázquez-Durán, M. C. Peña-Juárez, R. Vera-Graziano, M. I. Morales-Florido, B. Rodriguez-Perez, I. M. Rodriguez-Cruz and J. E. Miranda-Calderón, *International journal of molecular sciences*, 2023, **24**, 4289.
55. E. S. d. Silva, M. A. Polinarski, F. S. Bellucci, G. R. Burin, G. I. de Muniz and H. J. Alves.
56. E. Kalvand, H. Bakhshandeh, S. Nadri, M. Habibizadeh and K. Rostamizadeh, *Journal of Biomedical Materials Research Part A*, 2023, **111**, 1838-1849.
57. S. Benamer Oudih, D. Tahtat, A. Nacer Khodja, M. Mahlous, Y. Hammache, A. E. Guittoum and S. Kebbouche Gana, *Polymer Engineering & Science*, 2023, **63**, 1011-1021.
58. S. K. Shukla, A. K. Mishra, O. A. Arotiba and B. B. Mamba, *International journal of biological macromolecules*, 2013, **59**, 46-58.
59. P. Das, Université Paul Sabatier-Toulouse III; Universiteit Twente (Enschede …, 2018.
60. J. J. Wilson and L. Thomas, *bioRxiv*, 2023, 2023.2004. 2002.534760.
61. T. Tayebi, A. Baradaran-Rafii, A. Hajifathali, A. Rahimpour, H. Zali, A. Shaabani and H. Niknejad, *Scientific Reports*, 2021, **11**, 7060.
62. A. R. Sadeghi-Avalshahr, S. Nokhasteh, A. M. Molavi, N. Mohammad-Pour and M. Sadeghi, *International journal of molecular sciences*, 2020, **21**, 2311.
63. S. Gautam, S. D. Purohit, H. Singh, A. K. Dinda, P. D. Potdar, C. Sharma, C.-F. Chou and N. C. Mishra, *Materials Today Communications*, 2023, **34**, 105237.
64. M. Valente, J. Puiggalí, L. J. Del Valle, G. Titolo and M. Sambucci, *Polymers*, 2021, **13**, 2751.
65. S. Sharif, J. Ai, M. Azami, J. Verdi, M. A. Atlasi, S. Shirian and A. Samadikuchaksaraei, *Journal of Biomedical Materials Research Part B*, **106**, 1578-1586.
66. F. Asghari, D. R. Faradonbeh, Z. V. Malekshahi, H. Nekounam, B. Ghaemi, Y. Yousefpoor, H. Ghanbari and R. Faridi-Majidi, *Carbohydrate Polymers*, **278**, 118926-118926.
67. X. Xie, D. Li, C.-M. Su, W. Cong, X. Mo, G.-G. Hou and C. Wang, *Journal of Biomedical Nanotechnology*, **15**, 1267-1279.
68. T. Prasad, E. Shabeena, D. Vinod, T. Kumary and P. Anil Kumar, *Journal of Materials Science: Materials in Medicine*, 2015, **26**, 1-13.
69. S. L. Levengood, A. E. Erickson, F.-c. Chang and M. Zhang, *Journal of Materials Chemistry B*, 2017, **5**, 1822-1833.
70. S.-M. Jung, G. H. Yoon, H. C. Lee and H. S. Shin, *Journal of Biomaterials Science, Polymer Edition*, 2015, **26**, 252-263.
71. O. Ozkan and H. T. Sasmazel, *Journal of Nanoscience and Nanotechnology*, 2018, **18**, 2415-2421.
72. H. Chen, J. Huang, J. Yu, S. Liu and P. Gu, *International journal of biological macromolecules*, 2011, **48**, 13-19.
73. Z. Mousavi Nejad, A. Zamanian, M. Saeidifar, H. R. Vanaei and M. Salar Amoli, *Polymers*, 2021, **13**, 4442.
74. P. X. Ma and J.-W. Choi, *Tissue engineering*, 2001, **7**, 23-33.
75. S. Jin, J. Li, J. Wang, J. Jiang, Y. Zuo, Y. Li and F. Yang, *International journal of nanomedicine*, 2018, **13**, 4591.
76. M. EzEldeen, J. Loos, Z. Mousavi Nejad, M. Cristaldi, D. Murgia, A. Braem and R. Jacobs, *Eur Cell Mater*, 2021, **41**, 485-501.
77. B. Abinaya, T. P. Prasith, B. Ashwin, S. Viji Chandran and N. Selvamurugan, *Biotechnology Journal*, 2019, **14**, 1900171.
78. S. Ranganathan, K. Balagangadharan and N. Selvamurugan, *International journal of biological macromolecules*, 2019, **133**, 354-364.

79. N. Thuaksuban, T. Nuntanaranont, W. Pattanachot, S. Suttapreyasri and L. K. Cheung, *Biomedical Materials*, 2011, **6**, 015009.
80. S.-M. Mousavi, Z. M. Nejad, S. A. Hashemi, M. Salari, A. Gholami, S. Ramakrishna, W.-H. Chiang and C. W. Lai, *Membranes*, 2021, **11**, 702.
81. J. Zhu, H. Ye, D. Deng, J. Li and Y. Wu, *Journal of Biomaterials Applications*, 2020, **34**, 1282-1293.
82. A. Hashemi, M. Ezati, J. Mohammadnejad, B. Houshmand and S. Faghihi, *International Journal of Nanomedicine*, 2020, **15**, 4471.
83. L. Jiating, J. Buyun and Z. Yinchang, *BioMed research international*, 2019, **2019**.
84. W. Mu, Z. Wang, C. Ma, Y. Jiang, N. Zhang, K. Hu, L. Li and Z. Wang, *Pharmacological research*, 2018, **129**, 462-474.
85. D. Jhala, H. Rather and R. Vasita, *Biomaterials science*, 2016, **4**, 1584-1595.
86. S.-S. Hashemi, A. A. Mohammadi, S.-S. Rajabi, P. Sanati, A. Rafati, M. Kian and Z. Zarei, *BioImpacts: BI*, 2023, **13**, 275.
87. S. Ge, X. Zhu, C. Zhang, D. Jia, W. Shang, C. Ding, J. Yang and Y. Feng, *Molecules*, 2022, **27**, 8832.
88. M. I. Hassan, T. Sun and N. Sultana, *Journal of Nanomaterials*, 2014, **2014**.
89. T. Sun, T. H. Khan and N. Sultana, *Journal of Nanomaterials*, 2014, **2014**.
90. L. H. Chong, N. Z. Zarith and N. Sultana, 2015.
91. H. She, X. Xiao and R. Liu, *Journal of materials science*, 2007, **42**, 8113-8119.
92. S. Deepthi, K. Jeevitha, M. N. Sundaram, K. Chennazhi and R. Jayakumar, *Chemical Engineering Journal*, 2015, **260**, 478-485.
93. D. Poddar, P. Jain, S. Rawat and S. Mohanty, *Carbohydrate Polymers*, 2021, **259**, 117501.
94. S. C. Neves, L. S. M. Teixeira, L. Moroni, R. L. Reis, C. A. Van Blitterswijk, N. M. Alves, M. Karperien and J. F. Mano, *Biomaterials*, 2011, **32**, 1068-1079.
95. J. Schagemann, H. Chung, E. Mrosek, J. Stone, J. Fitzsimmons, S. O'driscoll and G. Reinholz, *Journal of Biomedical Materials Research Part A: An Official Journal of The Society for Biomaterials, The Japanese Society for Biomaterials, and The Australian Society for Biomaterials and the Korean Society for Biomaterials*, 2010, **93**, 454-463.
96. R. Asgarpour, E. Masaeli and S. Kermani, *Polymers for Advanced Technologies*, **32**, 4721-4732.
97. G. Bahcecioglu, B. Bilgen, N. Hasirci and V. Hasirci, *Biomaterials*, **218**, 119361-119361.
98. F. Sharifi, S. M. Atyabi, D. Norouzian, M. Zandi, S. Irani and H. Bakhshi, *International Journal of Biological Macromolecules*, **115**, 243-248.
99. R. Asgarpour, E. Masaeli and S. Kermani, *Polymers for Advanced Technologies*, 2021, **32**, 4721-4732.
100. G. Bahcecioglu, B. Bilgen, N. Hasirci and V. Hasirci, *Biomaterials*, 2019, **218**, 119361.
101. W. L. Miller and J. C. Burnett, Jr., *Rheum Dis Clin North Am*, 1990, **16**, 251-260.
102. N. Desbuards, G. Y. Rochefort, D. Schlecht, M. C. Machet, J. M. Halimi, V. Eder, J. M. Hyvelin and D. Antier, *Thromb Haemost*, 2007, **98**, 614-620.
103. P. Chandra and A. Atala, *Clin Sci (Lond)*, 2019, **133**, 1115-1135.
104. H. Bergmeister, N. Seyidova, C. Schreiber, M. Strobl, C. Grasl, I. Walter, B. Messner, S. Baudis, S. Frohlich, M. Marchetti-Deschmann, M. Griesser, M. di Franco, M. Krssak, R. Liska and H. Schima, *Acta Biomater*, 2015, **11**, 104-113.
105. L. E. Freed, G. C. Engelmayr, Jr., J. T. Borenstein, F. T. Moutos and F. Guilak, *Adv Mater*, 2009, **21**, 3410-3418.
106. L. Soletti, Y. Hong, J. Guan, J. J. Stankus, M. S. El-Kurdi, W. R. Wagner and D. A. Vorp, *Acta Biomater*, 2010, **6**, 110-122.
107. C. M. Vaz, S. van Tuijl, C. V. Bouten and F. P. Baaijens, *Acta Biomater*, 2005, **1**, 575-582.
108. T. H. Nguyen and B. T. Lee, *Sci Technol Adv Mater*, 2012, **13**, 035002.

109. W. Mrowczynski, D. Mugnai, S. de Valence, J. C. Tille, E. Khabiri, M. Cikirikcioglu, M. Moller and B. H. Walpoth, *J Vasc Surg*, 2014, **59**, 210-219.
110. J. Lee, J. J. Yoo, A. Atala and S. J. Lee, *Biomaterials*, 2012, **33**, 6709-6720.
111. G. Pitarresi, C. Fiorica, F. S. Palumbo, S. Rigogliuso, G. Ghersi and G. Giammona, *J Biomed Mater Res A*, 2014, **102**, 1334-1341.
112. K. Madhavan, W. H. Elliott, W. Bonani, E. Monnet and W. Tan, *J Biomed Mater Res B Appl Biomater*, 2013, **101**, 506-519.
113. W. Gong, D. Lei, S. Li, P. Huang, Q. Qi, Y. Sun, Y. Zhang, Z. Wang, Z. You and X. Ye, *Biomaterials*, 2016, **76**, 359-370.
114. K. Madhavan, W. H. Elliott, W. Bonani, E. Monnet and W. Tan, *Journal of Biomedical Materials Research Part B: Applied Biomaterials*, 2013, **101**, 506-519.
115. A. Agrawal, B. H. Lee, S. A. Irvine, J. An, R. Bhuthalingam, V. Singh, K. Y. Low, C. K. Chua and S. S. Venkatraman, *Int J Biomater*, 2015, **2015**, 434876.
116. W. Gong, D. Lei, S. Li, P. Huang, Q. Qi, Y. Sun, Y. Zhang, Z. Wang, Z. You, X. Ye and Q. Zhao, *Biomaterials*, 2016, **76**, 359-370.
117. X. Ran, Z. Ye, M. Fu, Q. Wang, H. Wu, S. Lin, T. Yin, T. Hu and G. Wang, *Macromol Biosci*, 2019, **19**, e1800189.
118. J. Shi, S. Chen, L. Wang, X. Zhang, J. Gao, L. Jiang, D. Tang, L. Zhang, A. Midgley, D. Kong and S. Wang, *J Biomed Mater Res B Appl Biomater*, 2019, **107**, 2040-2049.
119. S. E. Kim, S. I. Jeong, K. M. Shim, K. Jang, J. S. Park, Y. M. Lim and S. S. Kang, *Polymers (Basel)*, 2022, **14**.
120. Q. P. Pham, U. Sharma and A. G. Mikos, *Tissue Eng*, 2006, **12**, 1197-1211.
121. G. Cittadella Vigodarzere and S. Mantero, *Front Physiol*, 2014, **5**, 362.
122. Y. Dzenis, *Science*, 2004, **304**, 1917-1919.
123. S. Agarwal, J. H. Wendorff and A. Greiner, *Adv Mater*, 2009, **21**, 3343-3351.
124. B. P. Chan and K. W. Leong, *Eur Spine J*, 2008, **17 Suppl 4**, 467-479.
125. A. Cipitria, A. Skelton, T. R. Dargaville, P. D. Dalton and D. W. Hutmacher, *Journal of Materials Chemistry*, 2011, **21**, 9419-9453.
126. S. H. Ku and C. B. Park, *Biomaterials*, 2010, **31**, 9431-9437.
127. H. Sun, L. Mei, C. Song, X. Cui and P. Wang, *Biomaterials*, 2006, **27**, 1735-1740.
128. D. B. Gurevich, P. D. Nguyen, A. L. Siegel, O. V. Ehrlich, C. Sonntag, J. M. Phan, S. Berger, D. Ratnayake, L. Hersey, J. Berger, H. Verkade, T. E. Hall and P. D. Currie, *Science*, 2016, **353**, aad9969.
129. B.-K. Lee, Y. M. Ju, J.-G. Cho, J. D. Jackson, S. J. Lee, A. Atala and J. J. Yoo, *Biomaterials*, 2012, **33**, 9027-9036.
130. J. L. Lowery, N. Datta and G. C. Rutledge, *Biomaterials*, 2010, **31**, 491-504.
131. Y. Liu, G. Zhou, Z. Liu, M. Guo, X. Jiang, M. B. Taskin, Z. Zhang, J. Liu, J. Tang, R. Bai, F. Besenbacher, M. Chen and C. Chen, *Sci Rep*, 2017, **7**, 8197.
132. T. Navaei, P. B. Milan, A. Samadikuchaksaraei, H. R. Davari, J. G. Hardy and M. Mozafari, *J Tissue Eng Regen Med*, 2021, **15**, 78-87.
133. V. Perez-Puyana, P. Villanueva, M. Jimenez-Rosado, F. de la Portilla and A. Romero, *Polymers (Basel)*, 2021, **13**.
134. J. L. Aparicio-Collado, N. Garcia-San-Martin, J. Molina-Mateo, C. Torregrosa Cabanilles, V. Donderis Quiles, A. Serrano-Aroca and I. S. R. Sabater, *Colloids Surf B Biointerfaces*, 2022, **214**, 112455.
135. C. A. Charitidis, D. A. Dragatogiannis, E. Milioni, M. Kaliva, M. Vamvakaki and M. Chatzinikolaidou, *Materials*, 2019, **12**, 150.
136. A. Repanas, H. Zernetsch, D. Mavrilas and B. Glasmacher, *Pneumologie*, 2014, **68**, A86.

137. N. Mei, G. Chen, P. Zhou, X. Chen, Z.-Z. Shao, L.-F. Pan and C.-G. Wu, *Journal of biomaterials applications*, 2005, **19**, 323-339.
138. T. Navaei, P. B. Milan, A. Samadikuchaksaraei, H. R. Davari, J. G. Hardy and M. Mozafari, *Journal of Tissue Engineering and Regenerative Medicine*, 2021, **15**, 78-87.
139. T.-J. Wang, I. J. Wang, F.-R. Hu and T.-H. Young, *Cornea*, 2016, **35**.
140. S. Shi, Z. Zhang, Z. Luo, J. Yu, R. Liang, X. Li and H. Chen, *Scientific Reports*, 2015, **5**, 11337.
141. T.-H. Young, I. J. Wang, F.-R. Hu and T.-J. Wang, *Colloids and Surfaces B: Biointerfaces*, 2014, **116**, 403-410.
142. F. Jafari, S. N. Khorasani, F. Alihosseini, D. Semnani, S. Khalili and R. E. J. P. S. Neisiany, Series B, 2020, **62**, 290-298.
143. D. Zhang, N. Ni, J. Chen, Q. Yao, B. Shen, Y. Zhang, M. Zhu, Z. Wang, J. Ruan, J. Wang, X. Mo, W. Shi, J. Ji, X. Fan and P. Gu, *Scientific Reports*, 2015, **5**, 14326.
144. A. Sepahvandi, M. Eskandari and F. Moztarzadeh, *Materials Science and Engineering: C*, 2016, **66**, 306-314.
145. T.-H. Young, I.-J. Wang, F.-R. Hu and T.-J. Wang, *Colloids and Surfaces B: Biointerfaces*, 2014, **116**, 403-410.
146. A. Sepahvandi, M. Eskandari and F. Moztarzadeh, *Materials Science and Engineering: C*, 2016, **66**, 306-314.
147. S. Shi, Z. Zhang, Z. Luo, J. Yu, R. Liang, X. Li and H. Chen, *Scientific reports*, 2015, **5**, 11337.
148. T.-J. Wang, I.-J. Wang, J.-N. Lu and T.-H. J. M. v. Young, 2012, **18**, 255.
149. C. P. Jiménez-Gómez and J. A. Cecilia, *Molecules (Basel, Switzerland)*, 2020, **25**.
150. R. C. Cheung, T. B. Ng, J. H. Wong and W. Y. Chan, *Marine drugs*, 2015, **13**, 5156-5186.
151. H. Chen, X. Fan, J. Xia, P. Chen, X. Zhou, J. Huang, J. Yu and P. Gu, *Int J Nanomedicine*, 2011, **6**, 453-461.
152. T.-J. Wang, I. J. Wang, S. Chen, Y.-H. Chen and T.-H. Young, *Colloids and Surfaces B: Biointerfaces*, 2012, **90**, 236-243.
153. H. Chen, J. Huang, J. Yu, S. Liu and P. Gu, *International journal of biological macromolecules*, 2011, **48**, 13-19.
154. Y.-H. Wang, T.-H. Young and T.-J. Wang, *Experimental Eye Research*, 2019, **185**, 107679.
155. H. Aung, A. Sivakumar, S. Gholami, S. Venkateswaran and B. Gorain, *Nanotechnology-Based Targeted Drug Delivery Systems for Lung Cancer*, 2019, 1-20.
156. H. Tebyanian, A. Karami, M. R. Nourani, E. Motavallian, A. Barkhordari, M. Yazdanian and A. Seifalian, *Journal of Cellular Physiology*, 2019, **234**, 19256-19270.
157. F. S. Rezaei, A. Khorshidian, F. M. Beram, A. Derakhshani, J. Esmaeili and A. Barati, *RSC advances*, 2021, **11**, 19508-19520.
158. F. Koch, O. Thaden, S. Conrad, K. Tröndle, G. Finkenzeller, R. Zengerle, S. Kartmann, S. Zimmermann and P. Koltay, *Journal of The Mechanical Behavior of Biomedical Materials*, **130**, 105219-105219.
159. C. Mahoney, K. X. D. Conklin and J. W. N. Bhattarai.
160. S. N. Bhatia, G. H. Underhill, K. S. Zaret and I. J. Fox, *Science translational medicine*, 2014, **6**, 245sr242-245sr242.
161. V. Vilas-Boas, A. Cooreman, E. Gijbels, R. Van Campenhout, E. Gustafson, S. Ballet, P. Annaert, B. Cogliati and M. Vinken, *Advances in Pharmacology*, 2019, **85**, 1-30.
162. U. Ruman, S. Fakurazi, M. J. Masarudin and M. Z. Hussein, *International journal of nanomedicine*, 2020, **15**, 1437.
163. A. S. Rahman, F. J. M. Shamrat, Z. Tasnim, J. Roy and S. A. Hossain, *International Journal of Scientific & Technology Research*, 2019, **8**, 419-422.

164. S. Li, A. Saviano, D. J. Erstad, Y. Hoshida, B. C. Fuchs, T. Baumert and K. K. Tanabe, *Journal of Clinical Medicine*, 2020, **9**, 3817.
165. E. S. Mirdamadi, D. Kalhori, N. Zakeri, N. Azarpira and M. Solati-Hashjin, *Tissue Engineering Part B: Reviews*, 2020, **26**, 145-163.
166. C. D. Hoemann, J. R. González, J. Guzmán-Morales, G. Chen, E. J. Dil and B. D. Favis, *Bioactive Materials*, 2022, **10**, 430-442.
167. H. Huang, S. Oizumi, N. Kojima, T. Niino and Y. Sakai, *Biomaterials*, 2007, **28 26**, 3815-3823.
168. Z. Feng, X.-h. Chu, N. P. Huang, T. Wang, Y.-C. Wang, X. Shi, Y. Ding and Z.-Z. Gu, *Biomaterials*, 2009, **30 14**, 2753-2763.
169. K. H. Lee, S.-J. Shin, C.-b. Kim, J. K. Kim, Y. W. Cho, B. G. Chung and S. H. Lee, *Lab on a chip*, 2010, **10 10**, 1328-1334.
170. Z.-Q. Feng, X. Chu, N.-P. Huang, T. Wang, Y. Wang, X. Shi, Y. Ding and Z.-Z. Gu, *Biomaterials*, 2009, **30**, 2753-2763.
171. X.-H. Chu, X.-L. Shi, Z.-Q. Feng, J.-Y. Gu, H.-Y. Xu, Y. Zhang, Z.-Z. Gu and Y.-T. Ding, *Biomaterials*, 2009, **30**, 4533-4538.
172. P. S. Bakshi, D. Selvakumar, K. Kadirvelu and N. Kumar, *International journal of biological macromolecules*, 2020, **150**, 1072-1083.
173. T. S. Demina, M. G. Drozdova, C. Sevrin, P. Compère, T. A. Akopova, E. Markvicheva and C. Grandfils, *Molecules*, 2020, **25**, 1949.
174. Y. Qiu, Z. Mao, Y. Zhao, J. Zhang, Q. Guo, Z. Gou and C. Gao, *Macromolecular Research*, 2012, **20**, 283-291.
175. F. Ghahremanzadeh, F. Alihosseini and D. Semnani, *International Journal of Biological Macromolecules*, 2021, **174**, 278-288.
176. R. Thomas, A. Kanso and J. R. Sedor, *Prim Care*, 2008, **35**, 329-vii.
177. S. C. Leong and T. L. Sirich, *Toxins (Basel)*, 2016, **8**.
178. S. Xiong, Y. Lyu, A. Davenport and K. Choy, *Nanomaterials*, 2021, **11**, 2247.
179. N. Ismail, A. Venault, J.-P. Mikkola, D. Bouyer, E. Drioli and N. Tavajohi Hassan Kiadeh, *Journal of Membrane Science*, 2020, **597**, 117601.
180. J. P. Zambon, R. S. Magalhaes, I. Ko, C. L. Ross, G. Orlando, A. Peloso, A. Atala and J. J. Yoo, *World J Nephrol*, 2014, **3**, 24-30.
181. M. Abecassis, S. T. Bartlett, A. J. Collins, C. L. Davis, F. L. Delmonico, J. J. Friedewald, R. Hays, A. Howard, E. Jones, A. B. Leichtman, R. M. Merion, R. A. Metzger, F. Pradel, E. J. Schweitzer, R. L. Velez and R. S. Gaston, *Clin J Am Soc Nephrol*, 2008, **3**, 471-480.
182. A. Eftekhari, S. Maleki Dizaj, E. Ahmadian, A. Przekora, S. M. Hosseiniyan Khatibi, M. Ardalan, S. Zununi Vahed, M. Valiyeva, S. Mehraliyeva, R. Khalilov and M. Hasanzadeh, *Materials (Basel)*, 2021, **14**.
183. S. B. Jing, L. Li, D. Ji, Y. Takiguchi and T. Yamaguchi, *J Pharm Pharmacol*, 1997, **49**, 721-723.
184. N. Nagano, H. Yoshimoto, T. Nishitoba, H. Sato, S. Miyata, M. Kusaka, S. B. Jing and T. Yamaguchi, *Nihon Yakurigaku Zasshi*, 1995, **106**, 123-133.
185. I. N. Chiang, W.-C. Huang, C.-Y. Huang and Y.-S. Pu, *Journal of biomedical materials research. Part B, Applied biomaterials*, 2016, **106**.
186. J. Gao, R. Liu, J. Wu, Z. Liu, J. Li, J. Zhou, T. Hao, Y. Wang, Z. Du, C. Duan and C. Wang, *Biomaterials*, 2012, **33**, 3673-3681.
187. C. P. Jiménez-Gómez and J. A. Cecilia, *Molecules*, 2020, **25**, 3981.
188. B. Başkapan and A. Callanan, *Tissue Engineering and Regenerative Medicine*, 2021, **19**.
189. T. P. Burton, A. Corcoran and A. Callanan, *Biomed Mater*, 2017, **13**, 015006.
190. J. Sun, X. Liu, Z. Chen, L. Jiang, M. Yuan and M. Yuan, *Journal*, 2022, **15**.
191. J. Sun, X. Liu, Z. Chen, L. Jiang, M. Yuan and M. Yuan, *Materials*, 2022, **15**, 1591.

192. M. Simşek, M. Capkın, A. Karakeçili and M. Gümüşderelioğlu, *J Biomed Mater Res A*, 2012, **100**, 3332-3343.
193. M. J. P. Biggs, R. G. Richards and M. J. Dalby, *Nanomedicine : nanotechnology, biology, and medicine*, 2010, **6 5**, 619-633.
194. T. A. Suter and A. Jaworski, *Science*, 2019, **365**, eaaw8231.
195. A. Lavorato, S. Raimondo, M. Boido, L. Muratori, G. Durante, F. Cofano, F. Vincitorio, S. Petrone, P. Titolo and F. Tartara, *International Journal of Molecular Sciences*, 2021, **22**, 572.
196. C. Y. Poetera and D. Abimanyu, *Bali Medical Journal*, 2021, **10**, 927-934.
197. M. P. Prabhakaran, J. R. Venugopal, T. T. Chyan, L. B. Hai, C. K. Chan, A. Y. Lim and S. Ramakrishna, *Tissue Engineering Part A*, 2008, **14**, 1787-1797.
198. A. Cooper, N. Bhattarai and M. Zhang, *Carbohydrate polymers*, 2011, **85**, 149-156.
199. C. Liao, J. Huang, S. Sun, B. Xiao, N. Zhou, D. Yin and Y. Wan, *Reactive and Functional Polymers*, 2013, **73**, 149-159.
200. H. Baniasadi, A. R. SA and S. Mashayekhan, *International journal of biological macromolecules*, 2015, **74**, 360-366.
201. T. Gordon, E. Udina, V. M. Verge and E. I. P. de Chaves, *Motor control*, 2009, **13**, 412-441.
202. M. Choi, N. Hasan, J. Cao, J. Lee, S. P. Hlaing and J.-W. Yoo, *International journal of biological macromolecules*, 2020, **142**, 680-692.
203. N. Saderi, M. Rajabi, B. Akbari, M. Firouzi and Z. Hassannejad, *Journal of Materials Science: Materials in Medicine*, 2018, **29**, 1-10.
204. Y. Pooshidani, N. Zoghi, M. Rajabi, M. Haghbin Nazarpak and Z. Hassannejad, *Journal of Materials Science: Materials in Medicine*, 2021, **32**, 1-12.
205. E. Kijeńska-Gawrońska, T. Bolek, M. Bil and W. Swieszkowski, *Journal of Materials Chemistry B*, 2019, **7**, 4509-4519.
206. H. Afrash, N. Nazeri, P. Davoudi, R. FaridiMajidi and H. Ghanbari, *Biointerface Res. Appl. Chem*, 2021, **11**, 12606-12617.
207. K. Nawrotek, M. Mąkiewicz and D. Zawadzki, *Polymers*, 2021, **13**, 775.
208. Á. Serrano-Aroca, C. D. Vera-Donoso and V. Moreno-Manzano, *Int J Mol Sci*, 2018, **19**, 1796.
209. S. Baker, G. Rohman, J. Southgate and N. Cameron, *Biomaterials*, 2009, **30**, 1321-1328.
210. Z. Zhou, H. Yan, Y. Liu, D. Xiao, W. Li, Q. Wang, Y. Zhao, K. Sun, M. Zhang and M. Lu, *Regen Med*, 2018, **13**, 331-342.
211. Z. Zhou, H. Yan, Y. Liu, D. Xiao, W. Li, Q. Wang, Y. Zhao, K. Sun, M. Zhang and M. Lu, *Regenerative Medicine*, 2018, **13**, 331-342.
212. E. Bilensoy, C. Sarisozen, G. Esendağlı, A. Doğan, Y. Aktaş, M. Sen and N. Mungan, *International journal of pharmaceutics*, 2009, **371**, 170-176.
213. N. Erdoğar, A. B. Iskit, N. A. Mungan and E. Bilensoy, *J Microencapsul*, 2012, **29**, 576-582.
214. G. Orlando, J. E. García-Arrarás, T. Soker, C. Booth, B. Sanders, C. L. Ross, P. De Coppi, A. C. Farney, J. Rogers and R. J. Stratta, *Digestive and Liver Disease*, 2012, **44**, 714-720.
215. D. Zhao, S. Yu, B. Sun, S. Gao, S. Guo and K. Zhao, *Polymers (Basel)*, 2018, **10**, 462.
216. M. S. Rodríguez and L. E. Albertengo, *Biosci Biotechnol Biochem*, 2005, **69**, 2057-2062.
217. G. B. Cardoso, A. B. Machado-Silva, M. Sabino, A. R. Santos, Jr. and C. A. Zavaglia, *Biomatter*, 2014, **4**.
218. M. C. Bonferoni, C. Caramella, L. Catenacci, B. Conti, R. Dorati, F. Ferrari, I. Genta, T. Modena, S. Perteghella, S. Rossi, G. Sandri, M. Sorrenti, M. L. Torre and G. Tripodo, *Pharmaceutics*, 2021, **13**, 1341.
219. S. C. Neves, L. S. Moreira Teixeira, L. Moroni, R. L. Reis, C. A. Van Blitterswijk, N. M. Alves, M. Karperien and J. F. Mano, *Biomaterials*, 2011, **32**, 1068-1079.

220. Y.-C. Chiu, H.-Y. Fang, T.-T. Hsu, C.-Y. Lin and M.-Y. Shie, *Journal of Endodontics*, 2017, **43**, 923-929.
221. B. Divband, B. Pouya, M. Hassanpour, M. Alipour, R. Salehi, R. Rahbarghazi, S. Shahi, Z. Aghazadeh and M. Aghazadeh, *BioMed Research International*, 2022, **2022**, 5401461.
222. M. G. C. Sousa, M. R. Maximiano, R. A. Costa, T. M. B. Rezende and O. L. Franco, *Expert Opinion on Drug Delivery*, 2020, **17**, 919-930.
223. Y. Zhang, R. Jiang, L. Lei, Y. Yang and T. Hu, *J Appl Oral Sci*, 2022, **30**, e20210349-e20210349.
224. K. S. Moharir, M. Kurakula, V. Kale, E.-R. Kenawy, S. Murtuja, M. N. Ahsan, M. S. Hasnain and A. K. Nayak, in *Chitosan in Biomedical Applications*, eds. M. S. Hasnain, S. Beg and A. K. Nayak, Academic Press, 2022, DOI: https://doi.org/10.1016/B978-0-12-821058-1.00004-6, pp. 75-110.
225. M. Masoudi Rad, S. Nouri Khorasani, L. Ghasemi-Mobarakeh, M. P. Prabhakaran, M. R. Foroughi, M. Kharaziha, N. Saadatkish and S. Ramakrishna, *Materials Science and Engineering: C*, 2017, **80**, 75-87.
226. F. Tondnevis, M. A. Ketabi, R. Fekrazad, A. Sadeghi and M. M. Abolhasani, *Journal of Biomimetics, Biomaterials and Biomedical Engineering*, 2019, **42**, 39-50.
227. M. Alipour, Z. Aghazadeh, M. Hassanpour, M. Ghorbani, R. Salehi and M. Aghazadeh, *Stem Cells International*, 2022, **2022**, 7583489.
228. R. F. Bombaldi de Souza and Â. M. Moraes, *Journal of Materials Science*, 2022, **57**, 2924-2940.
229. M. Ezati, H. Safavipour, B. Houshmand and S. Faghihi, *Progress in Biomaterials*, 2018, **7**, 225-237.
230. T. Ouchi, G. Orsini, A. George and M. Kajiya, *Frontiers in Cell and Developmental Biology*, 2022, **10**.
231. S. Patil, M. Rayasa, H. Mahajan, R. Wagh and S. Gattani, *Pharma Times*, 2006, **38**, 25-28.
232. L. Mazzarino, L. Coche-Guérente, P. Labbé, E. Lemos-Senna and R. Borsali, *J Biomed Nanotechnol*, 2014, **10**, 787-794.
233. L. Mazzarino, R. Borsali and E. Lemos-Senna, *J Pharm Sci*, 2014, **103**, 3764-3771.
234. M. Ezati, H. Safavipour, B. Houshmand and S. Faghihi, *Progress in biomaterials*, 2018, **7**, 225-237.
235. F. P. S. Guastaldi, T. Takusagawa, J. L. G. C. Monteiro, Y. He, Q. Ye and M. J. Troulis, in *Bone Tissue Engineering: Bench to Bedside Using 3D Printing*, eds. F. P. S. Guastaldi and B. Mahadik, Springer International Publishing, Cham, 2022, DOI: 10.1007/978-3-030-92014-2_5, pp. 93-119.
236. Y. Yang, H. Wu, Q. Fu, X. Xie, Y. Song, M. Xu and J. Li, *Materials & Design*, 2022, **214**, 110394.
237. Y. Takeoka, K. Matsumoto, D. Taniguchi, T. Tsuchiya, R. Machino, M. Moriyama, S. Oyama, T. Tetsuo, Y. Taura, K. Takagi, T. Yoshida, A. Elgalad, N. Matsuo, M. Kunizaki, S. Tobinaga, T. Nonaka, S. Hidaka, N. Yamasaki, K. Nakayama and T. Nagayasu, *PLoS One*, 2019, **14**, e0211339.
238. R. Dorati, A. De Trizio, S. Marconi, A. Ferrara, F. Auricchio, I. Genta, T. Modena, M. Benazzo, A. Benazzo, G. Volpato and B. Conti, *Macromol Biosci*, 2017, **17**.
239. R. Dorati, S. Pisani, G. Maffeis, B. Conti, T. Modena, E. Chiesa, G. Bruni, U. M. Musazzi and I. Genta, *Carbohydr Polym*, 2018, **199**, 150-160.
240. K. S. Vasanthan, V. Srinivasan, V. Mathur, P. Agarwal, N. Negi and S. Kumari, *Journal of Materials Research*, 2022, **37**, 88-113.
241. S. D. Kim, I. G. Kim, H. N. Tran, H. Cho, G. Janarthanan, I. Noh and E. J. Chung, *Tissue Eng Part A*, 2021, **27**, 1490-1502.
242. A. O'Connor and C. O'Moráin, *Dig Dis*, 2014, **32**, 186-191.
243. J. C. Hemmeter, *Diseases of the Stomach: Their Special Pathology, Diagnosis, and Treatment* Nabu Press Philadelphia : P. Blakiston Son & Co., 1897, 2010.
244. R. A. Rothwell, M. S. Pridham and G. A. Thomson, Berlin, Heidelberg, 2010.
245. T. Kimura and K. Higaki, *Biol Pharm Bull*, 2002, **25**, 149-164.
246. J. F. Pinto, *Int J Pharm*, 2010, **395**, 44-52.

247. T. Hussain, M. Ijaz, R. Shamim, K. Hussain, N. Abbas, A. Hussain, J. A. Griessinger and N. I. Bukhari, *AAPS PharmSciTech*, 2020, **21**, 58.
248. T. Hussain, A. Hussain, R. Shamim, M. Shehzad, D. M. Danish, K. Hussain and N. Bukhari, *LATIN AMERICAN JOURNAL OF PHARMACY*, 2015, **34**, 1849-1857.
249. Y. Fu and W. J. Kao, *Expert Opin Drug Deliv*, 2010, **7**, 429-444.
250. C. M. Dekaney, A. S. Gulati, A. P. Garrison, M. A. Helmrath and S. J. Henning, *Am J Physiol Gastrointest Liver Physiol*, 2009, **297**, G461-470.
251. J. H. Hageman, M. C. Heinz, K. Kretzschmar, J. van der Vaart, H. Clevers and H. J. G. Snippert, *Dev Cell*, 2020, **54**, 435-446.
252. G. Gaucher, P. Satturwar, M. C. Jones, A. Furtos and J. C. Leroux, *Eur J Pharm Biopharm*, 2010, **76**, 147-158.
253. A. Almeida, D. Silva, V. Gonçalves and B. Sarmento, *Drug Deliv Transl Res*, 2018, **8**, 387-397.
254. C. Gu, V. Le, M. Lang and J. Liu, *Colloids and Surfaces B: Biointerfaces*, 2014, **116**, 745-750.
255. M. Hadjianfar, D. Semnani and J. Varshosaz, *Polymers for Advanced Technologies*, 2018, **29**.
256. E. Zakhem, S. Raghavan, R. R. Gilmont and K. N. Bitar, *Biomaterials*, 2012, **33**, 4810-4817.
257. A. Gupta, D. S. Vara, G. Punshon, K. M. Sales, M. C. Winslet and A. M. Seifalian, *Journal*, 2009, **54**, 221-229.
258. C. Gu, V. Le, M. Lang and J. Liu, *Colloids and Surfaces B: Biointerfaces*, 2014, **116**, 745-750.
259. N. C. Huang, K. W. Teng, N. C. Huang, L. Y. Kang, K. Y. Fu, P. S. Hsieh, L. G. Dai and N. T. Dai, *Ann Plast Surg*, 2020, **84**, S116-s122.

Declaration of interests

☒The authors declare that they have no known competing financial interests or personal relationships that could have appeared to influence the work reported in this paper.

☐The authors declare the following financial interests/personal relationships which may be considered as potential competing interests:

Highlight

- Synthetic polymers and natural biomaterials are used to create specific scaffolds.
- Polycaprolactone has good mechanical but modest biological properties.
- Chitosan has strong biological but weak mechanical traits for tissue regeneration.
- Combining PCL and CS enhances scaffold fabrication for various tissues.
- PCL:CS-based scaffolds are key in evolving 3D frameworks for tissue engineering.